

**ACTIVITY MANAGEMENT ALGORITHM
FOR IMPROVING ENERGY EFFICIENCY
OF SMALL CELL BASE STATIONS IN 5G
HETEROGENEOUS NETWORKS**

A THESIS

SUBMITTED TO THE DEPARTMENT OF ELECTRICAL AND
ELECTRONICS ENGINEERING

AND THE GRADUATE SCHOOL OF ENGINEERING AND SCIENCE
OF BILKENT UNIVERSITY

IN PARTIAL FULFILLMENT OF THE REQUIREMENTS

FOR THE DEGREE OF

MASTER OF SCIENCE

By

Irmak Aykın

July, 2014

I certify that I have read this thesis and that in my opinion it is fully adequate, in scope and in quality, as a thesis for the degree of Master of Science.

Prof. Dr. Ezhan Karaşan(Advisor)

I certify that I have read this thesis and that in my opinion it is fully adequate, in scope and in quality, as a thesis for the degree of Master of Science.

Assoc. Prof. Dr. Nail Akar

I certify that I have read this thesis and that in my opinion it is fully adequate, in scope and in quality, as a thesis for the degree of Master of Science.

Assoc. Prof. Dr. İbrahim Körpeoğlu

Approved for the Graduate School of Engineering and Science:

Prof. Dr. Levent Onural
Director of the Graduate School

ABSTRACT

ACTIVITY MANAGEMENT ALGORITHM FOR IMPROVING ENERGY EFFICIENCY OF SMALL CELL BASE STATIONS IN 5G HETEROGENEOUS NETWORKS

Irmak Aykın

M.S. in Electrical and Electronics Engineering

Supervisor: Prof. Dr. Ezhan Kardeş

July, 2014

Heterogeneous networks (HetNets) are proposed in order to meet the increasing demand for next generation cellular wireless networks, but they also increase the energy consumption of the base stations. In this thesis, an activity management algorithm for improving the energy efficiency of HetNets is proposed. A smart sleep strategy is employed for the operator deployed pico base stations to enter sleep and active modes. According to that strategy, when the number of users exceeds the turn on threshold, the pico node becomes active and when the number of users drop below the turn off threshold, it goes into sleep mode. Mobile users dynamically enter and leave the cells, triggering the activation and deactivation of pico base stations. The performance of the system is examined for three different cellular network architectures: cell on edge (COE), uniformly distributed cells (UDC) and macro cell only network (MoNet). Two different user distributions are considered: uniform and hotspot. The effects of number of hotspot users and sleep energies of pico nodes on the energy efficiency are also investigated. The proposed activity management algorithm increases the energy efficiency, measured in bits/J, by 20%. The average bit rates achieved by HetNet users increase by 29% compared with the MoNet architecture. Thus, the proposed activity control algorithm increases the spectral efficiency of the network while consuming the energy more efficiently.

Keywords: heterogeneous networks, sleep mode, LTE, activity management, algorithm, energy efficiency, small cell, green communications.

ÖZET

5G HETEROJEN AĞLARDA KÜÇÜK HÜCRE BAZ İSTASYONLARININ ENERJİ VERİMLİLİĞİ ARTTIRIMI İÇİN AKTİVİTE YÖNETİMİ ALGORİTMASI

Irmak Aykın

Elektrik Elektronik Mühendisliği, Yüksek Lisans

Tez Yöneticisi: Prof. Dr. Ezhan Karaşan

Temmuz, 2014

Yeni nesil kablosuz hücresel ağların artan ihtiyacını karşılamak için tasarlanan heterojen ağlar (HetNets), aynı zamanda bu sistemlerin enerji tüketimini de arttırmaktadır. Bu tez kapsamında, heterojen ağların enerji verimliliğini geliştirebilmek için bir aktivite yönetim algoritması önerilmiştir. Bu amaçla, akıllı uyku stratejisi kullanılmış ve operatör tarafından yerleştirilmiş piko düğümlerin uyku veya aktif moda geçmesi yönetilmiştir. Bu stratejiye göre, kullanıcı sayısı açılış eşik değerinin üstüne çıktığında piko düğüm aktif hale gelir. Öte yandan, kullanıcı sayısı kapanış eşik değerinin altına düştüğünde piko düğüm tekrardan uyku moduna geçer. Mobil kullanıcılar dinamik bir şekilde hücrelerin kapsama alanına girip çıkarak piko baz istasyonlarını etkinleştirir veya etkisizleştirir. Sistem performansı, kenarlarda bulunan hücreler (COE), düzgün olarak dağıtılmış hücreler (UDC) ve sadece makro hücrenin bulunduğu ağ (MoNet) topolojileri için araştırılmıştır. Kullanıcı dağılımı için ise gelişigüzel ve popüler nokta durumları incelenmiştir. Ayrıca, popüler noktaların kullanıcı sayısının ve piko düğümlerin harcadığı uyku enerjilerinin enerji verimliliği üzerine etkileri araştırılmıştır. Önerilen aktivite yönetim algoritması enerji verimliliğini bits/J cinsinden %20'ye kadar arttırabilmektedir. Heterojen ağ kullanıcılarının ortalama veri hızı da sadece makro hücrenin bulunduğu ağa kıyasla %29 artmıştır. Sonuç olarak, önerilen aktivite kontrol algoritması, daha verimli bir enerji tüketimi sağlarken ağın spektral verimliliğini de arttırmaktadır.

Anahtar sözcükler: heterojen ağlar, uyku modu, LTE, aktivite yönetimi, algoritma, enerji verimliliği, küçük hücre, yeşil haberleşme.

To my beloved family

Acknowledgement

I would like to express my special thanks to my supervisor Prof. Ezhan Karařan for his valuable guidance and sharing his knowledge through every step of this thesis.

I also thank to Assoc. Prof. Nail Akar and Assoc. Prof. İbrahim K rpeođlu for their valuable contributions to my thesis defense committee.

I want to thank to Berk Akg n for all his support. Without him, this thesis could not be completed. I also thank to Erman Zaim, Ulař Turan and Bahar řahin for their motivational support through all my stressful moments. In addition, I thank to my cat, B cek, for keeping me awake at nights and pushing me to study.

Finally, for their valuable support in every step of my life, I am grateful to my mother, my father and the rest of my family. Without them, I would not be who I am today.

Contents

- 1 Introduction 1**

- 2 Background Information 5**
 - 2.1 Wireless vs. Wired Communication 5
 - 2.2 Cellular Networks 6
 - 2.3 Heterogeneous Networks 8
 - 2.4 Wireless Communication Properties 9
 - 2.4.1 Spectral Efficiency and Energy Efficiency 10
 - 2.5 Network Configurations 11
 - 2.6 Base Station Power Models 13
 - 2.6.1 Base Station Sleep Modes 15
 - 2.7 User Movements 16
 - 2.8 User Distributions 17

- 3 Proposed Activity Management Algorithm for Energy Efficiency 18**
 - 3.1 Problem Definition 18

3.2	5G Heterogeneous Networks	19
3.2.1	Dual Connectivity	19
3.2.2	Almost Blank Subframes	20
3.2.3	Fairness	20
3.3	Activity Management Algorithm	21
4	Simulation Results	25
4.1	Simulation Environment	25
4.1.1	Network Topology	25
4.1.2	User Distributions	26
4.1.3	Mobility Model	28
4.1.4	Activity Model	30
4.1.5	Channel Model	30
4.1.6	Energy Model	31
4.2	Simulation Results	32
4.2.1	Simulations without Activity Management	32
4.2.2	Simulations with Activity Management	37
5	Conclusion	65

List of Figures

2.1	Cellular Systems [13]	6
2.2	Evolution of Cell Deployments	9
2.3	COE Configuration [5]	12
2.4	UDC Configuration	13
2.5	Load Dependent Power Model for a Typical LTE eNB [26]	14
3.1	State Diagram of pico-eNBs	22
3.2	Flowchart of Activity Management Algorithm	23
3.3	Hysteresis Shape of Activity Model of pico-eNBs	24
4.1	COE Configuration Used in Simulations	26
4.2	Dissipated Power vs. Number of Users	34
4.3	Dissipated Power vs. Time for 150 Stationary Users	35
4.4	Dissipated Power vs. Time for 150 Users with a Maximum Speed of 5 m/slot	35
4.5	Dissipated Power vs. Time for 150 Users with a Maximum Speed of 10 m/slot	36

4.6	Dissipated Power vs. Time for 150 Users with a Maximum Speed of 20 m/slot	36
4.7	Number of Active Pico eNBs vs. T_a	39
4.8	EE vs. T_a for MoNet, UDC and COE with $P_{sleep} = 0W$	40
4.9	EE vs. T_a for MoNet, UDC, COE, UDC w/o Macro and COE w/o Macro with $P_{sleep} = 0W$	41
4.10	EE vs. T_a for MoNet, UDC and COE with $P_{sleep} = 8.6W$	42
4.11	EE vs. T_a for MoNet, UDC, COE, UDC w/o Macro and COE w/o Macro with $P_{sleep} = 8.6W$	42
4.12	Histogram of bit rates achieved by MoNet users for $T_a = 2, 8$ and 12	43
4.13	Histogram of bit rates achieved by COE users for $T_a = 2, 8$ and 12	44
4.14	Histogram of bit rates achieved by UDC users for $T_a = 2, 8$ and 12	44
4.15	EE vs. T_a for MoNet, UDC, COE, UDC w/o Macro and COE w/o Macro with $P_{sleep} = 0W$ and $N_h = 500$	46
4.16	EE vs. T_a for MoNet, UDC, COE, UDC w/o Macro and COE w/o Macro with $P_{sleep} = 2W$ and $N_h = 500$	46
4.17	EE vs. T_a for MoNet, UDC, COE, UDC w/o Macro and COE w/o Macro with $P_{sleep} = 4W$ and $N_h = 500$	47
4.18	EE vs. T_a for MoNet, UDC, COE, UDC w/o Macro and COE w/o Macro with $P_{sleep} = 6W$ and $N_h = 500$	47
4.19	EE vs. T_a for MoNet, UDC, COE, UDC w/o Macro and COE w/o Macro with $P_{sleep} = 8.6W$ and $N_h = 500$	48
4.20	EE vs. T_a for MoNet, UDC, COE, UDC w/o Macro and COE w/o Macro with $P_{sleep} = 0W$ and $N_h = 250$	49

4.21	EE vs. T_a for MoNet, UDC, COE, UDC w/o Macro and COE w/o Macro with $P_{sleep} = 0W$ and $N_h = 750$	49
4.22	EE vs. T_a for MoNet, UDC, COE, UDC w/o Macro and COE w/o Macro with $P_{sleep} = 8.6W$ and $N_h = 250$	50
4.23	EE vs. T_a for MoNet, UDC, COE, UDC w/o Macro and COE w/o Macro with $P_{sleep} = 8.6W$ and $N_h = 750$	50
4.24	Histogram of bit rates achieved by MoNet users for $T_a = 5, 21$ and 27 , and $N_h = 500$	52
4.25	Histogram of bit rates achieved by COE Users for $T_a = 5, 21$ and 27 , and $N_h = 500$	52
4.26	Histogram of bit rates achieved by UDC Users for $T_a = 5, 21$ and 27 , and $N_h = 500$	53
4.27	EE vs. time for MoNet, UDC, COE, UDC w/o Macro and COE w/o Macro with $P_{sleep} = 0W$ and $N_h = 500$	55
4.28	EE vs. time for MoNet, UDC, COE, UDC w/o Macro and COE w/o Macro with $P_{sleep} = 8.6W$ and $N_h = 500$	55
4.29	Number of Users Served by Pico and Macro Cells vs. Time in UDC	57
4.30	Number of Users Served by Pico and Macro Cells vs. Time in COE	57
4.31	EE vs. time for $P_{sleep} = 0W$ and $T_a = 5$	59
4.32	EE vs. time for $P_{sleep} = 0W$, $T_a = 9$ and $T_d = 4$	59
4.33	EE vs. time for $P_{sleep} = 0W$ and $T_a = 9$	60
4.34	EE vs. time for $P_{sleep} = 0W$ and $T_a = 12$	60
4.35	EE vs. time for $P_{sleep} = 8.6W$ and $T_a = 5$	62
4.36	EE vs. time for $P_{sleep} = 8.6W$, $T_a = 9$ and $T_d = 4$	62

4.37 EE vs. time for $P_{sleep} = 8.6W$ and $T_a = 9$	63
4.38 EE vs. time for $P_{sleep} = 8.6W$ and $T_a = 12$	63

List of Tables

2.1	Power Model Parameters for Different Base Station Types [27] . .	15
4.1	Power Model Parameters for Different Base Station Types [32] . .	31
4.2	Energy Consumption Parameters for Various Base Station Types [32]	32
4.3	Initial Simulation Parameters [5]	33
4.4	EE, Bit Rate and Dissipated Energy Values for Various Thresholds (T_a)	38

Chapter 1

Introduction

The term Heterogeneous Network (HetNet) indicates the use of multiple types of access nodes/base stations in a cellular wireless network. A Wide Area Network (WAN) can use macro evolved node Bs (eNBs), together with low-power eNBs such as micro, pico and femto as base stations. The large macro cells provide basic coverage, while small cells boost capacity and/or extend the range of the cellular network. Macro base stations are large cell towers that can climb as high as 75 meters and can cover an area with diameter of up to 16 kilometers; whereas, micro cells are generally employed in suburban areas and provide a coverage diameter of less than 2 kilometers. On the other hand, pico cells cover areas of a diameter around 225 meters and are typically used for indoor applications; whereas, femto base stations are about the size of a Wi-Fi router and can typically support 2 to 4 simultaneous mobile phone calls [1]. Heterogeneous networks are seen as a promising way to meet the increasing demand for mobile broadband traffic in next generation cellular networks [2]. That is why, while a 2G or 3G deployment typically consists of multisector macro base stations only, with 4G and 5G cellular networks using LTE Advanced, HetNet deployment model which consists of small cells with micro, pico and femto base stations on top of macro base stations will be used [3].

However, with every eNB turning on, we encounter fixed offset power independent from the number of users being served, and that offset power is comparable

to, or even larger than, the load dependent power. That is why, activating small cells all the time, for a small number of users, is energy inefficient. We can increase the spectral efficiency as the number of active small cells increase, but then, we may consume an excessive amount of energy. According to [4], in 2020, the population of small cells is estimated to be around 100 million with 500 million mobile users. The power consumption of a typical small cell base station is around 50 W. Then, 100 million always active small cells in 2020 will consume approximately 44 TWh. This energy corresponds to the annual electricity consumption of roughly 10 million people with a total cost of about \$8 billion. Thus, it is crucial for small cell base stations to have some kind of a sleep strategy to save energy. If a power control mechanism is employed, the cost savings corresponding to the energy savings of HetNets are expected to be \$1.4 - \$1.6 billion in 2020 [5]. In addition, we can significantly reduce the CO₂ emissions, using a power control mechanism.

There are several suggestions to improve the energy efficiency of heterogeneous networks. Previous work in these areas can be briefly summarized as follows: [5] proposes an energy-efficient deployment of the cells where the small cell base stations are arranged around the edge of the reference macro cell, and the deployment is referred to as cell-on-edge (COE) deployment. The proposed deployment ensures an increase in the network spectral and energy efficiencies by facilitating cell edge mobile users with small cells. However, entirely coordinated small cell deployment is not a realistic scenario, and also COE does not improve the energy efficiency for mobile users with random movements. [6] introduces active/sleep (on/off) modes in macro cell base stations and investigate the performance. However, it is risky to turn on/off macro eNB, since it provides the main coverage. [7] shows that the energy efficiency of the two-tier networks with orthogonal spectrum deployment is better than that with co-channel spectrum deployment; thus, it is better not to allocate the same frequency to small and macro cells. [8] suggests switching off unnecessary cells to adapt actual traffic demand, but do not give details of its implementation. On the other hand, [9] introduces energy-efficient sleep mode algorithms for small cell base stations in

a bid to reduce cellular networks' power consumption. It gives detailed explanations of several sleep mode algorithms, but do not compare their performances in detail. [10] also introduces two node sleep modes operating on fast and intermediate time scales respectively, in order to exploit short and longer idle periods of the nodes. The introduced sleep modes are Micro DTX and Pico sleep; thus, it basically suggests different types of sleep modes for different types of small cells.

In this thesis, a smart sleep strategy is employed for improving energy efficiency in small cell base stations. When the number of users exceeds the turn on threshold, the pico node becomes active and when the number of users drop below the turn off threshold, it goes into sleep mode. As mobile users dynamically enter and leave the cells, they trigger the activation and deactivation of pico base stations. Two thresholds should be sufficiently far. Otherwise, when they are too close, the base station may oscillate between the two modes. And since the base station cannot serve a user right after being turned on, this oscillation causes delay and wasted energy. Thus, the proposed activity management algorithm has a hysteresis characteristic.

On the other hand, when the users' motions are not random, i.e., they move according to a hotspot model so as to enter and leave pico cells in groups, the HetNet model becomes more beneficial. Because, in that model, the number of users per pico cell increases and in return, the effect of offset power of the base station decreases. Also, in that case, using only one threshold may be sufficient, since the pico-eNBs do not turn on and off quite often and the probability of oscillations between two modes is very low. We show in the thesis that use of a single threshold in the hotspot user model does not significantly decrease the energy efficiency.

In this thesis, the energy-efficient small cell deployment model in [5] is used, together with other well-known deployment models, such as uniformly distributed cells (UDC) and macro cell only network (MoNet). In addition to [5], the performance of this model is investigated for the case with mobile hotspot users. Similar to [8], an algorithm that allows unnecessary small cells to turn off is proposed. The performance of this algorithm is evaluated in terms of energy efficiency and

spectral efficiency. According to our simulation results, the proposed activity management algorithm increases the energy efficiency in terms of $bits/J$ by 20%. We can also provide a bit rate up to 5.88×10^5 b/s to HetNet users where the users served by MoNet can get at most 5.28×10^5 b/s, which corresponds to an increase in bit rate by 10%. In the case of hotspot users, the bit rate provided by HetNet can get as high as 6.8×10^5 b/s, which is an increase by 29% compared with MoNet.

The rest of this thesis is organized as follows. In Chapter 2, the related background information is provided. The differences between wired and wireless communication is explained. The evolutions of cellular networks and heterogeneous networks are described. In addition, wireless communication properties are explained and related network configurations, base station power consumption models, user movement models and distributions are outlined.

In Chapter 3, a scheduling problem with the goal of maximizing the overall energy efficiency is introduced and the related background information is explained. Then, the proposed activity management algorithm and the employed hotspot user model are described in detail.

In Chapter 4, the simulation environment including the network topology, user distributions, mobility, activity, energy and channel models is explained. Then the simulation results are provided with detailed explanations.

Finally, in Chapter 5, the problem and proposed solutions are summarized and the deductions of the results are presented. Then, the thesis is concluded.

Chapter 2

Background Information

2.1 Wireless vs. Wired Communication

Wireless communication is the information exchange between two or more devices without using conducting wires [11]. Most wireless systems, such as two-way radios and cellular telephones, use radio waves for communication. Wired communication, on the other hand, is the data transmission with the use of wires and cables. Today's television transmission is an example of wired communication. The main advantage of wireless systems is their flexibility, i.e., they allow users to be mobile during communication. However, there are two aspects of wireless communication that make it a challenging problem. First one is fading, which is the attenuation affecting a signal over certain propagation media. This attenuation may either be due to the small-scale effect of multipath fading, as well as larger-scale effects such as path loss and shadowing by obstacles. Second, there is considerable interference between wireless users, since they share the same medium, unlike wired users that have their own isolated links. The interference can be between transmitters communicating with the same receiver (e.g., uplink of a cellular system), between signals from a single transmitter to multiple receivers (e.g., downlink of a cellular system), or between different transmitterreceiver pairs (e.g., interference between users in different cells) [12].

2.2 Cellular Networks

Today, perhaps the most commonly used wireless systems are cellular networks. A cellular network consists of a large number of wireless subscribers with cellular telephones, which can be used in cars, in buildings, on the street, or almost anywhere. There are also several fixed base-stations, which are organized to provide coverage of the subscribers. The area where the communication with the base station can be established is called a cell. Cells are usually assumed to be hexagonal regions with the base station being in the middle, and larger regions are assumed to be broken up into a hexagonal lattice of cells as seen from Figure 2.1 [13].

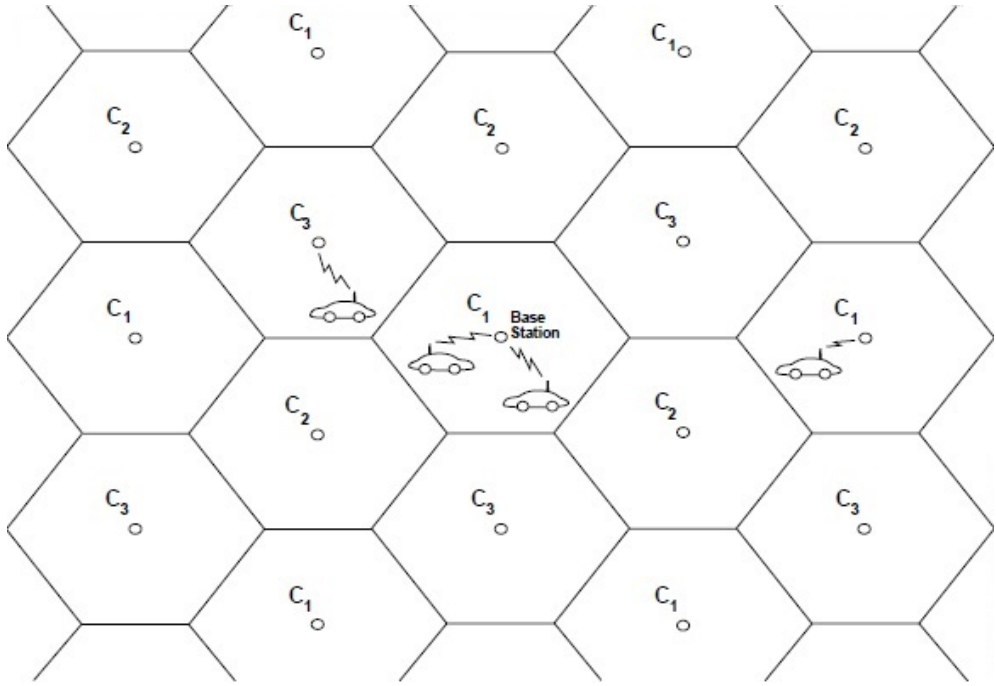


Figure 2.1: Cellular Systems [13]

Evolution of cellular networks has now reached its fourth generation. The cellular wireless generation (G) generally refers to a change in the fundamental

nature of the service. The first generation mobile systems used analog transmission since they were primarily designed before the widespread use of digital communications.

In 1G, the forward channel (downlink) was used for transmissions from the base stations to mobile users, using frequencies between 869-894 MHz. Transmissions from mobile users to base station, on the other hand, occurred on the reverse channel (uplink), using frequencies between 824-849 MHz. Traffic was multiplexed onto an FDMA (frequency division multiple access) system. Frequency modulation (FM) technique was used by Advanced Mobile Phone System and Total Access Communication System for radio transmission [14] [15].

Unlike 1G, second-generation (2G) systems used digital multiple access technology, such as TDMA (time division multiple access) and CDMA (code division multiple access). As a result, compared to 1G systems, 2G systems provided higher spectrum efficiency, better data services, and more advanced roaming.

3G does not consist of a single standard; in fact, it is a family of standards that all work together. The organization called 3rd Generation Partnership Project (3GPP) has defined a mobile system that fulfils the IMT-2000 standard. 3G networks allow service providers to offer users more advanced services while attaining greater network capacity by means of improved spectral efficiency. 3G telecommunication networks support services that enable users to transfer data at a rate of at least 2Mbps.

The first successful trial of 4G was made in 2005. In 4G networks, users are capable of selecting the wireless systems to use 4G services. In existent GSM systems, base stations periodically broadcast messages to mobile users for subscription. However, this procedure becomes more complex in 4G heterogeneous networks because of the differences in wireless technologies. Thus, terminal mobility is a requirement in 4G infrastructure to provide wireless services at anytime and anywhere. Terminal mobility allows mobile users to travel across boundaries of wireless networks. There are two main issues in terminal mobility: location management and handoff management. With location management, a mobile terminal is tracked and located by the system for a potential connection. Location

management involves managing all the information about the roaming terminals, such as current and previous cells and authentication information. On the other hand, handoff management preserves the continuing communications when the terminal roams [16].

The Third Generation Partnership Project (3GPP) had specified the basis of the future Long Term Evolution (LTE) Advanced, the 3GPP candidate for 4G, standards [17]. The target values of peak spectrum efficiency for LTE Advanced systems were set to 30 bps/Hz for downlink and 15 bps/Hz for uplink channels. Improved multiple-input multiple-output (MIMO) channel transmission techniques and extensive coordination between multiple cell sites called coordinated multipoint (CoMP) transmission/reception were accepted as the key techniques for LTE, together with the multiple access schemes [18].

2.3 Heterogeneous Networks

With LTE Advanced, a new term Heterogeneous Network (HetNet) was introduced. HetNets have gained significant attention for their ability to optimize the system performance, especially for uneven user and traffic distributions. LTE networks were first based on homogeneous networks consisting of macro base stations that provided basic coverage. With the involvement of pico and femto base stations (eNBs), networks achieved significant improvement in terms of overall capacity and cell-edge performance. In HetNets, layers of low power pico or femto eNBs (evolved node B) that are deployed in a less planned manner are on top of the layer of planned high power macro eNBs [2]. Cellular systems in urban areas now generally use small cells for street level transmissions at much lower power [13]. Typical 2G/3G and 4G HetNet deployments can be seen from Figure 2.2 (a) and (b), respectively.

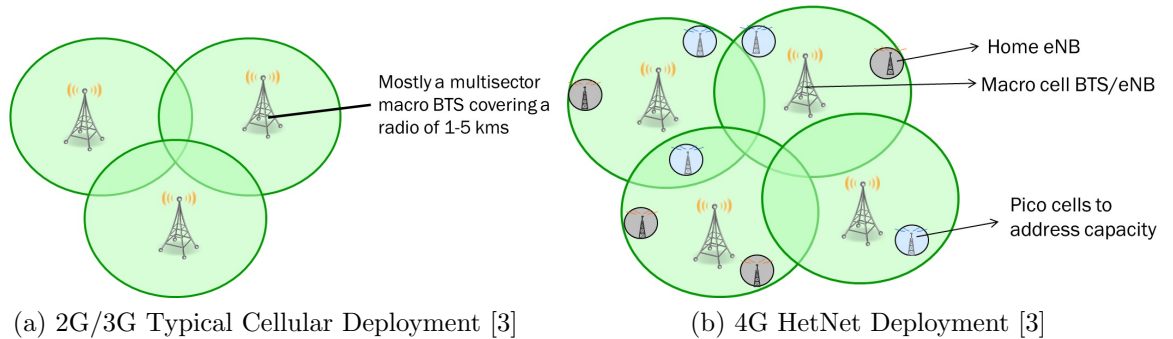


Figure 2.2: Evolution of Cell Deployments

However, the evolution of heterogeneous networks resulted in more complicated network designs. Since, mobile users pass through small cells more quickly than a macro cell; handoffs must be processed more quickly. Moreover, location management becomes harder, as there are more cells within a given area where a user can be located [13]. Energy management is also an important issue, since activating pico nodes all the time may be energy inefficient. Thus, small cell eNBs should have some kind of sleep strategy.

2.4 Wireless Communication Properties

In wireless systems, output power of the transmitter is different from the power received by the receiver. This is mainly due to path loss, shadowing and multipath fading. Path loss is usually expressed in dB. In its simplest form, the path loss can be calculated as

$$L = 10n \log_{10} d + C \quad (2.1)$$

where L is the path loss in decibels, n is the path loss exponent, d is the distance between the transmitter and the receiver, and C is a constant which accounts for system losses.

Experiments reported by Egli in 1957 showed that, for paths longer than a few hundred meters, the received power fluctuates with a log-normal distribution about the area-mean power. This fluctuation is due to shadowing and the probability density function (pdf) of the local-mean power is thus of the form shown as

$$f_{\bar{p}_{\log}}(\bar{p}_{\log}) = \frac{1}{\sqrt{2\pi}\sigma_s} \exp\left[-\frac{1}{2\sigma_s^2}(\bar{p}_{\log})^2\right] \quad (2.2)$$

where, σ_s is the logarithmic standard deviation of the shadowing, expressed in natural units.

Also, in wireless networks, the signal offered to the receiver contains not only a direct line-of-sight radio wave, but also a large number of reflected radio waves. The phases of the reflected waves are altered; thus, these reflected waves interfere with the direct wave, which causes significant degradation of the performance of the network known as multipath fading. Although channel fading is experienced as an unpredictable, stochastic phenomenon, powerful models such as Rician and Rayleigh Fading have been developed in order to accurately predict system performance [19].

2.4.1 Spectral Efficiency and Energy Efficiency

An important tool to analyse a network is the Quality of Service (QoS). QoS is the overall performance of a network, particularly the performance experienced by the users of the network. To quantitatively measure QoS, several related aspects of the network service are often considered, such as error rates, throughput, transmission delay and jitter. QoS can also be regarded as the ability to provide different priority to different applications, users, or data flows, or to guarantee a certain level of performance to a data flow. For example, a required bit rate, delay, jitter, packet dropping probability and/or bit error rate may be guaranteed [20]. In the context of HetNets, we consider two QoS parameters: energy efficiency which is measured in *bits/J* and the average bit rate achieved by users.

To calculate the bit rate that a mobile user gets, we use the Shannon's capacity

formula given by

$$C_i = w_i \log_2(1 + SNR_i) \quad (2.3)$$

where, w_i is the bandwidth of that user and SNR_i is the Signal to Noise Ratio of the user.

SNR that a user gets can be calculated by

$$SNR_i = \frac{P_t^{BS} PL_i(d_i) G_{BS} G_{MU} P_{shadow}}{kT w_i} \quad (2.4)$$

where P_t^{BS} is the transmit power of the base station, $PL_i(d_i)$ is the path loss the user experiences, G_{BS} and G_{MU} are antenna gains of base station and mobile user, P_{shadow} is the shadowing with log-normal distribution, T is the temperature in Kelvin and k is the Boltzmann constant. SNR value in the receiver should be above a certain threshold for the symbols to be accurately decoded.

Using these values and total consumed power, we can obtain the parameter bits per joule ($bits/J$), which is used as a metric for energy efficiency (EE). $bits/J$ is simply the ratio of the capacity to the rate of energy expenditure [21]. It can be seen as a special case of the capacity per unit cost [22]. We define EE as

$$EE = \frac{\sum_i C_i}{P_{tot}} \text{ bits}/J \quad (2.5)$$

where the summation in the numerator is the total capacity of the network and P_{tot} is the total consumed power.

2.5 Network Configurations

LTE networks were first based on homogeneous networks consisting of macro base stations that provided basic coverage. That network configuration, consisting of macro cells only, is called MoNet.

Now that heterogeneous networks are seen as a promising way to meet the increasing demand for mobile broadband traffic in cellular networks, new pico

nodes complement the macro nodes to provide higher capacity in areas with higher user density [23]. There are two widely used topologies for heterogeneous networks, namely cell on edge (COE) and uniformly distributed cells (UDC). In COE, small cells are located on the edge of the reference macro cell as in Figure 2.3. The main aim of the COE configuration is to provide capacity and coverage to cell edge mobile users by reducing the distance between the transmitter (mobile user in uplink) and the receiver (BS in uplink) [5]. This way, since the mobile users that experience largest path loss are allowed to transmit to nearest small cell, capacities of the cell edge users increase. That leads to the increase of the overall capacity. However, since the layers of low-power pico nodes are less well planned or even entirely uncoordinated, COE is not a very realistic topology.

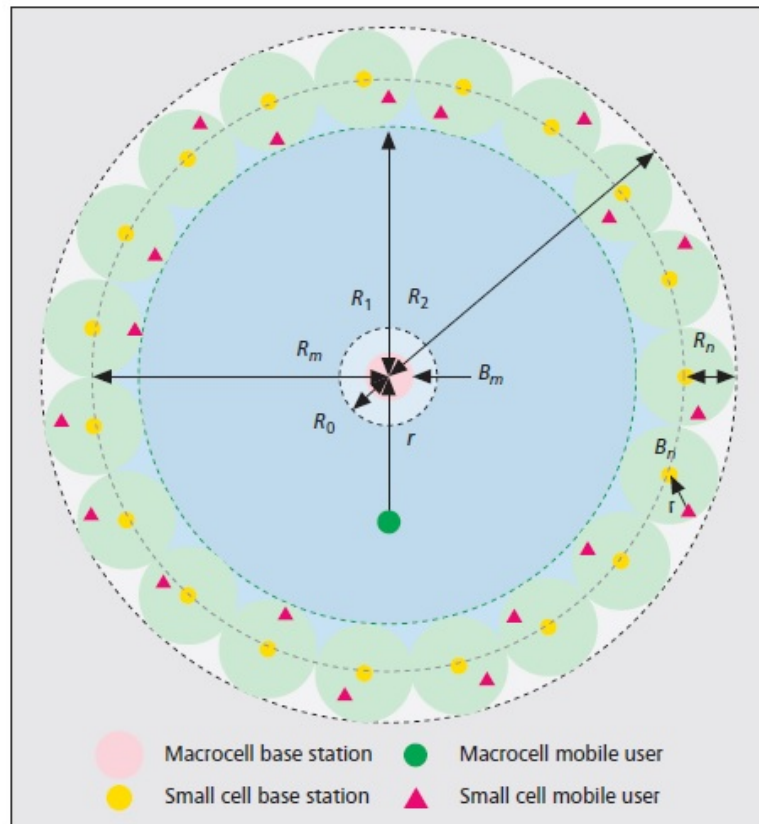


Figure 2.3: COE Configuration [5]

Alternative approach is UDC, where the small cells are uniformly distributed across the macro cells as shown in Figure 2.4 [5]. UDC may not improve the system’s capacity as much as COE, but it suits real life scenarios better.

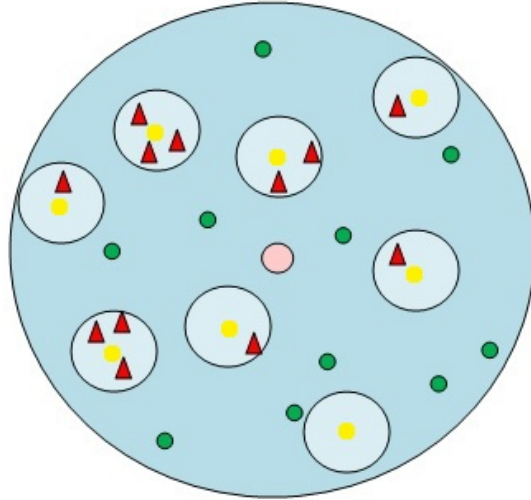


Figure 2.4: UDC Configuration

2.6 Base Station Power Models

Recent surveys on the energy consumption of cellular networks, including base stations (BSs), mobile terminals and the core network, show that around 80% of the energy required to run a cellular network is consumed at base stations [24]. The energy efficiency frameworks therefore focus on the base station power consumption.

The base station power model maps the RF output power radiated at the antenna elements, P_{out} , to the total supply power of a base station site, P_{in} . In an LTE downlink, the eNB load is proportional to the amount of utilized resources, comprising both data and control signals. More generally the base station load also depends on power control settings, in terms of the transmitted

spectral power density.

Figure 2.5 shows the principle characteristics of the proposed simplified estimate of an eNB power model for LTE. The detailed study of base station components in EARTH [25] has shown that there is large offset power consumption at zero load. As indicated in Figure 2.5, the relation between relative RF output power P_{out} and eNB power consumption P_{in} is approximated by the function

$$P_{in} = \begin{cases} N_{trx}(P_0 + \Delta_p P_{out}) & 0 < P_{out} \leq P_{max} \\ N_{trx} \cdot P_{sleep} & P_{out} = 0 \end{cases} \quad (2.6)$$

where N_{trx} is the number of transceiver chains (transceiver/receiver antennas per site), P_0 is the power consumption at the minimum non-zero output power, P_{max} is the maximum RF output power per component carrier and P_{out} is a fraction of it, and Δ_p is the slope of the load dependent power consumption.

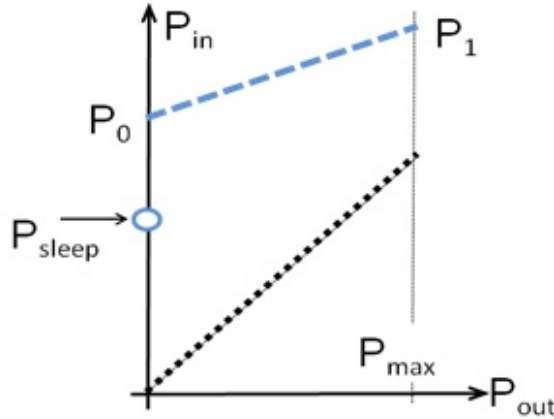


Figure 2.5: Load Dependent Power Model for a Typical LTE eNB [26]

The parameters of the linear power model for the base stations of interest are obtained by least squares curve fitting of the detailed model [25] and are listed in Table 2.1. The parameters are based on an LTE system with 2x10 MHz bandwidth and 2x2 MIMO configuration [26].

Table 2.1: Power Model Parameters for Different Base Station Types [27]

BS type	N_{TRX}	$P_{\text{max}}[\text{W}]$	$P_0[\text{W}]$	Δ_p	$P_{\text{sleep}}[\text{W}]$
Macro	6	20	130	4.7	75
Micro	2	6.3	56	2.6	39
Pico	2	0.13	6.8	4.0	4.3
Femto	2	0.05	4.8	8.0	2.9

2.6.1 Base Station Sleep Modes

There are several suggestions to base station sleep modes such as; small cell controlled sleep mode, core network controlled sleep mode and UE controlled sleep mode. In small cell controlled sleep mode, by using the existence of macro cell coverage, the small cell hardware can be enriched with a low-power sniffer capability that allows the detection of an active call from a UE. Then, the small cell can afford to disable its pilot transmissions and the associated radio processing when no active calls are being made by the UE in its coverage area. The sniffer-based sleep mode requires one macro cell small cell handover per connection; however, the benefits outweigh this [28]. In core network controlled sleep mode, different from the suggestion above, it is not required for the low-power sniffer in the small cell to detect active UEs. Alternatively, the transition of small cell from sleep to active state is controlled by the core network via the backhaul using a wake-up control message. The core network driven approach allows the possibility to take a centralized decision, based not only on a particular UE but also taking into account the macro cell traffic load. A third approach is to place the sleep mode control at the UE side, which can broadcast wake-up signals in order to wake up small cell BSs within its range. To implement this, the UE can broadcast periodic wake-up signals continuously so that any small cells in sleep mode will transition to active mode when the UE approaches it. This means that coverage provided by small cells follows a UE unit as it moves around and ensures that UE units are given small cell coverage whenever possible [9].

2.7 User Movements

A suitable model for defining user movements is the Brownian Motion Model. Brownian motion is the random motion of particles suspended in a fluid (a liquid or a gas) resulting from their collision with the quick atoms or molecules in the gas or liquid [29]. The term Brownian motion can also refer to the mathematical model used to describe such random movements. The mathematical model of Brownian motion has numerous real-world applications, like stock market fluctuations.

An elementary example of a 1D Brownian motion is the random walk on the integer number line, \mathbb{Z} , which starts at 0 and at each step moves $+1$ or -1 with equal probability. This walk can be illustrated as follows. A marker is placed at zero on the number line and a fair coin is flipped. If it lands on heads, the marker is moved one unit to the right. If it lands on tails, the marker is moved one unit to the left. After five flips, the marker could now be on $-5, -3, -1, 1, 3, 5$. With five flips, three heads and two tails, in any order, will land on -1 . There are 10 ways of landing on -1 (by flipping three heads and two tails), 10 ways of landing on 1 (by flipping three tails and two heads), 5 ways of landing on -3 (by flipping four heads and one tail), 5 ways of landing on 3 (by flipping four tails and one head), 1 way of landing on -5 (by flipping five heads), and 1 way of landing on 5 (by flipping five tails).

For the 2D illustration, we can imagine a drunkard walking randomly in an idealized city. The city is effectively infinite and arranged in a square grid, and at every intersection, the drunkard chooses one of the four possible routes (including the one he came from) with equal probability. Formally, this is a random walk on the set of all points in the plane with integer coordinates. The trajectory of this random walk is the collection of sites he visited [30].

For a map that is not arranged in a grid topology, 2D Brownian motion can be modelled as follows: the users randomly select a destination coordinate inside the map and a speed (between 0 and pre-determined maximum). At each

time slot, their positions are updated as $X = X_{prev} + V_x$ and $Y = Y_{prev} + V_y$. When they reach their destinations, they start the process again.

2.8 User Distributions

The users can be distributed within the network in two ways: uniform and non-uniform (hotspot). In uniform, user equipments (UEs) are randomly and uniformly distributed in the geographic coverage area of macro cells. On the other hand, in hotspot, a fraction of the total UEs are randomly placed within the coverage area low power cells and the remaining UEs are randomly and uniformly distributed within the macro cells [31].

Hotspot is a more realistic approach than purely uniform distribution since mobile users are not uniformly distributed in real life. Instead, the number of users is denser in areas such as schools, shopping malls and hospitals. Some hotspots may periodically turn on and off, depending on the time of the day. For instance, a hotspot may occur in a business centre between 8am - 5pm, whereas another may operate in a shopping mall between 10am - 10pm. The small cells serving a hotspot may require more bandwidth than a regular small cell, in order to maintain the required QoS.

In this chapter, we have provided the related background information. In the next chapter, an activity management problem that aims to maximize EE will be introduced and an activity management algorithm will be proposed.

Chapter 3

Proposed Activity Management Algorithm for Energy Efficiency

In this chapter, we discuss the activity control problem that defines the trade-off between energy efficiency and capacity. Then, the related background information is explained and activity management algorithm is described.

3.1 Problem Definition

Heterogeneous networks are seen as a promising way to meet the increasing demand for mobile broadband traffic in next generation cellular networks. The new pico-eNBs complement the macro-eNBs to provide higher capacity in areas with higher user density [23]. That is because, even though they allocate the user same bandwidth that macro-eNB allocates, since their coverage area is smaller, their signals face lower path loss. Thus, the SNRs that their users achieve, and bit rate in return, are larger. However, the pico-eNB power model which is given in Equation (2.6) suggests that with every eNB turning on, we encounter an offset power $N_{tx} \cdot P_0$, independent from the number of users being served. This offset power is comparable to, or even larger than, the user dependent power.

Thus, activating pico nodes all the time, for small number of users, is energy inefficient. Then, they should have some kind of sleep strategy. The pico-eNBs should be turned on and off in a way to maximize the overall EE, which is measured by *bits/J*. Also, there should be a sufficient number of users in a pico cell for adequate improvement of the total capacity. For these purposes, we propose an activity control mechanism which turns on and off pico-eNBs in order to save energy.

The proposed approach contains two thresholds, T_a and T_d , which are used for turning on and off the base stations, respectively. The activity management problem is defined as determining T_a and T_d in a way to increase the EE, where EE is defined in Equation (2.5).

3.2 5G Heterogeneous Networks

5G infrastructure has important properties that allow HetNets to operate flawlessly. In this section, some of these properties are explained and the fairness metric is discussed.

3.2.1 Dual Connectivity

The term dual connectivity is used to refer to operation where a given UE consumes radio resources provided by at least two different network points connected with non-ideal backhaul [32]. That way, it is possible for a user to switch from macro cell to pico cell almost instantly, without interrupting the current transmissions. Thus, when a pico-eNB is turned off or when a UE enters the coverage area of a pico-eNB, it can instantly begin to use the resources of the new cell.

3.2.2 Almost Blank Subframes

Transmissions from macro-eNBs inflicting high interference onto pico-eNBs users are periodically muted (stopped) during entire subframes, this way the pico-eNB users that are suffering from a high level of interference from the aggressor macro-eNB have a chance to be served. However this muting is not complete as certain control signals are still transmitted which are:

- Common reference symbols (CRS)
- Primary and secondary synchronization signals (PSS and SSS)
- Physical broadcast channel (PBCH)
- SIB-113 and paging with their associated PDCCH.

These control channels have to be transmitted even in the muted subframes to avoid radio link failure or for reasons of backwards compatibility, so muted subframes should be avoided in subframes where PSS, SSS, SIB-1 and paging are transmitted or in other words subframes #0, #1, #5 and #9. Since these muted subframes are not totally blank they are called Almost Blank Subframes (ABS). The basic idea is to have some subframes during which the macro-eNB is not allowed to transmit data allowing the range extension pico-eNB users, who were suffering from interference from the macro-eNB transmission, to transmit with better conditions [33].

3.2.3 Fairness

Among the fairness metrics such as max-min fairness, proportional fairness and α -fairness, we used equal bandwidth share that makes the users fair in terms of allocated bandwidth. The total allocated bandwidth of a macro cell is assumed to be W . All pico and macro eNBs are assumed to be transmitting in different frequencies as it eliminates co-channel interference and provides better performance [7], so some of that bandwidth is given to pico-eNBs. The total number of

users is assumed to be N and since they are fair in terms of allocated bandwidth, each user gets a bandwidth of W/N . Then, the bandwidth allocated to a cell is directly proportional with the number of users within that cell.

3.3 Activity Management Algorithm

In the first network model, transmission energies of eNBs have been determined only according to path loss and path loss has been determined according to the Free Space Propagation Model, where the parameters are obtained from [5]. The received signal power at a mobile user, from the desired eNB can be calculated by

$$P^{rx}(r) = P^{tx} \frac{K}{r^\alpha(1+r/g)^\beta} \quad (3.1)$$

If we reverse this equation, we can achieve the desired transmit power at the base station as

$$P^{tx}(r) = \min(P_{\max}, P_0 \frac{r^\alpha(1+r/g)^\beta}{K}) \quad (3.2)$$

where, r is the distance between user and base station, α and β are basic and additional path loss exponents, g is the breakpoint distance, K is the path loss constant, P_0 is the arbitrary cell-specific parameter that corresponds to the target signal-to-interference-plus-noise ratio, P_{\max} is the maximum transmit power and P_{rx} and P_{tx} are received and transmit powers, respectively [5].

If we assume that base stations do not consume any fixed energy when no users are connected to them, it is not necessary to have an activity management mechanism. On the other hand, if base stations can immediately start serving users when they are activated, the activity control mechanism can switch on and off the base stations as frequently as desired.

However, as given by the energy model shown in Equation (2.6), the base stations have some load independent fixed energy consumption. Moreover, they cannot start serving the users immediately after being turned on. Therefore, in

our more realistic network, the state diagram of pico-eNBs is modelled as shown in Figure 3.1. So, for a pico-eNB to turn on, it should first enter boot mode. In boot mode, a node cannot communicate with users, it only consumes some fixed energy, representing the energy consumed by the circuitry. Boot mode lasts for some slot time. In that time, users communicate with macro-eNB, as pico-eNB is not yet ready for transmission. Since macro-eNB never goes into a sleep mode, no boot mode is required for it.

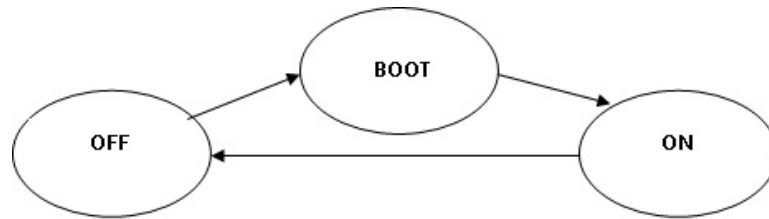


Figure 3.1: State Diagram of pico-eNBs

The main objective is to maximize the EE and thus, optimally decide the thresholds for a pico-eNB to turn on and turn off. They are meant to be optimum in the sense of energy usage and network capacity. We would like to turn the pico-eNBs on, in order to increase the capacity. However, we would also like to turn off under-utilized eNBs to decrease the consumed energy, as the eNBs consume high fixed powers. In addition, these two thresholds should be different. Otherwise, the node may oscillate between two modes, as the node cannot go from sleep to active mode instantly, and that causes delay and wasted energy. Thus, the flow chart of the activity management algorithm is given in Figure 3.2, where N_{pico} is the number of users within a pico cell. The behaviour of the activity management algorithm as a function of N_{pico} is depicted in Figure 3.3.

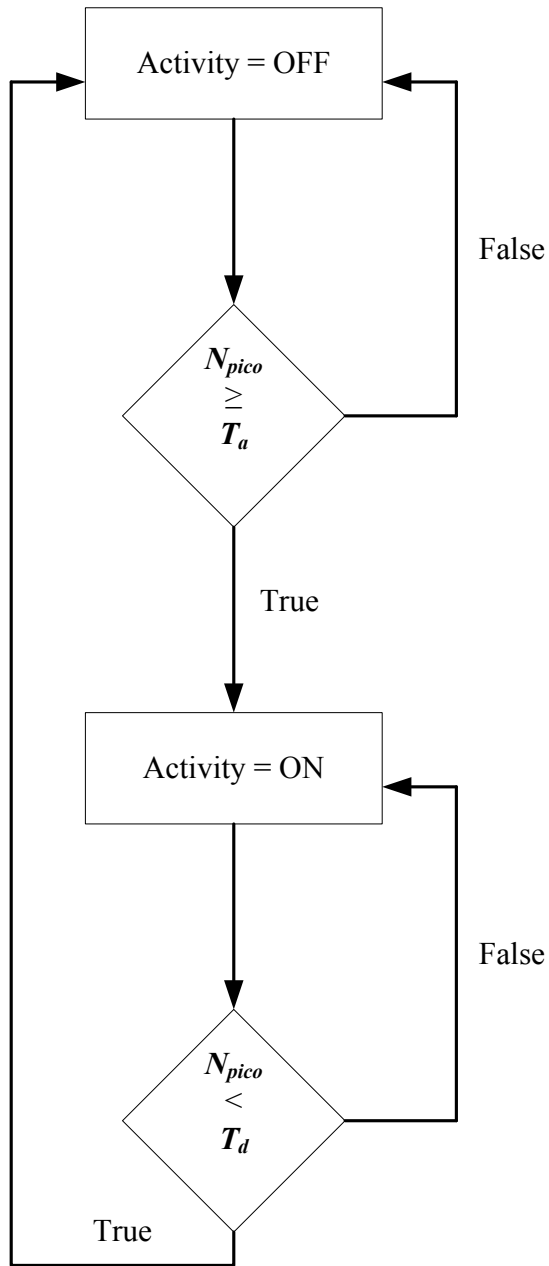


Figure 3.2: Flowchart of Activity Management Algorithm

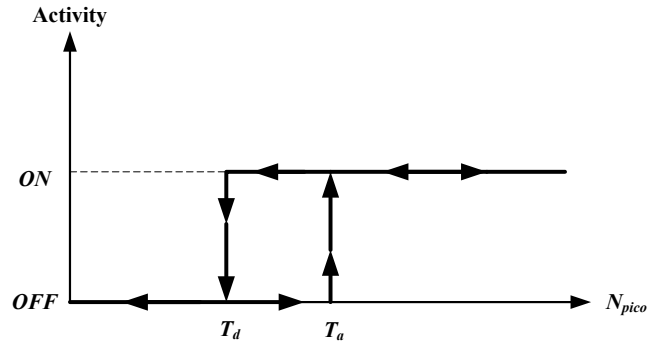


Figure 3.3: Hysteresis Shape of Activity Model of pico-eNBs

However, in the case that users do not enter and leave pico cells instantaneously, only one threshold may be sufficient, since in that case, the pico-eNB does not turn on and off quite often and the probability of oscillations is very low. In return, the location of the second threshold would not change the performance of the system.

In this chapter, we have introduced the problem of increasing EE and described the proposed activity management algorithm. In the next chapter, simulation environment including network topology, user distributions, mobility, activity, energy and channel models will be explained. Then, the simulation results will be provided and explained in detail.

Chapter 4

Simulation Results

In this chapter, simulation environment and parameters used are introduced. Then, simulation results are provided and obtained results are discussed in detail.

4.1 Simulation Environment

4.1.1 Network Topology

As mentioned in Chapter 3, there are 3 network configurations that we consider: COE, UDC and MoNet. There are 28 pico cells both in UDC and COE with coverage radius being 50m, whereas the coverage radius of macro cell is 500m. In real applications, the pico eNBs are planned to be placed in only concentration areas for optimum performance; thus, their number per macro cell can be larger or smaller than this value. The locations of pico eNBs in UDC configuration is random such that no two cells intersect. On the other hand, their locations in COE are specially designed so that they cover almost all areas at the edge of macro cell. The COE configuration that is used in simulations can be seen in Figure 4.1.

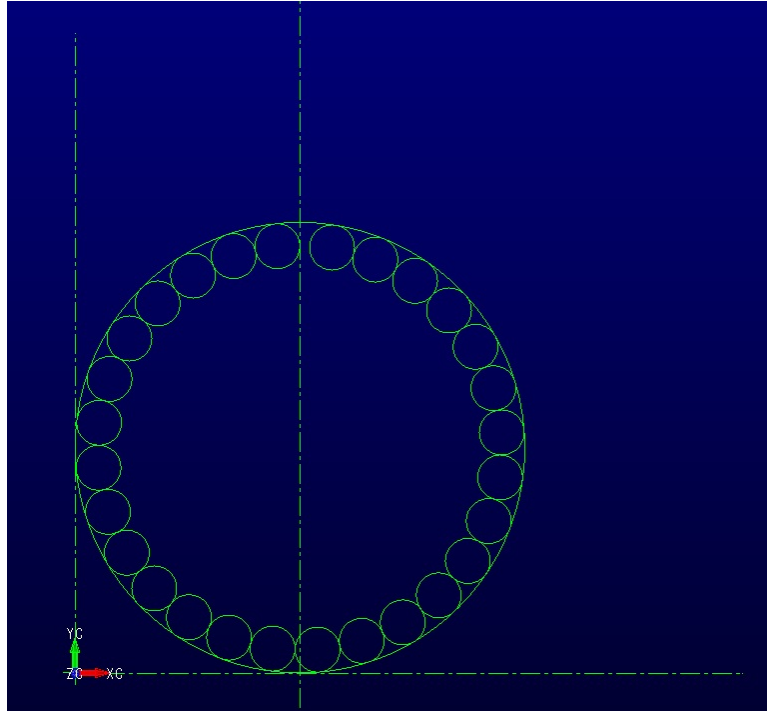


Figure 4.1: COE Configuration Used in Simulations

In the simulations, we have considered only one macro cell and it is placed so as to be tangential to the axes. Then, the pico cells are positioned in a manner that they would be tangential to both the macro cell and each other. After that, the locations of macro and pico eNBs are determined and used in simulations.

4.1.2 User Distributions

4.1.2.1 Uniform

In the uniform user distribution, the users are placed to their initial locations randomly. There are $N=1000$ users. For any pico cell, if the distance between UE and eNB is less than 50m, then the user is assumed to be within that pico cell. When the distance between the UE and eNB exceeds 50m, the user is

immediately served by macro eNB. No slot is wasted during this process, thanks to dual connectivity. In this case, since the users are distributed in a uniform manner, the maximum number of users that a pico cell can get is around 20. This number is a little low to see the benefits of the heterogeneous network.

In order to make a fair comparison between network configurations, the users are distributed and moved the same in all three cases. In other words, UDC, COE and MoNet configurations can be visualised as transparent layers and users are located below them. Thus, all configurations see the same users in same locations at all times.

4.1.2.2 Hotspot

EE of the users of pico cells may be sufficiently large. However, number of users in pico cells may be very small; since when the users are distributed randomly, their probability of being inside a pico cell is quite small. Thus, the overall effect of the pico cells would not be very significant. Then, to observe the benefit of the HetNet more, we should increase the number of users in pico cells. For that purpose, instead of distributing the users randomly, we should introduce a hotspot concept.

In hotspot scenario, there are N_h hotspot users and $N - N_h$ random users that act like in uniform case. All hotspot users are assigned a specific pico cell and work time during their creations. Then, initially, all users are again distributed randomly. When their assigned work time come, each user picks a random location from their allocated pico cell and starts moving towards it. In this case, when we have taken the number of hotspot users as 500, the maximum number of users that a pico cell can get is around 50, which is a sufficient number to see the benefits of heterogeneous network as shown by simulations.

However, since the cells are located in different places in UDC and COE, user distributions cannot be the same in hotspot scenario for UDC, COE and MoNet. Thus, to make a fair comparison, we have taken the UDC and COE hotspot user distributions for MoNet, as two different scenarios. In other words,

in these cases, MoNet can be visualized as a transparent layer on top of UDC and COE user distributions. Also, we named these two scenarios as MoNet with COE configuration and MoNet with UDC configuration. Naturally, MoNet with UDC configuration performs better than MoNet with COE configuration, since in the latter, macro eNB needs to serve many users at the edge of its coverage area.

4.1.3 Mobility Model

All users move according to the Brownian Motion Model, with different parameters. Uniform users choose a speed between 0 and 20 randomly and at each slot, they update their positions as $X = X_{prev} + V_x$ and $Y = Y_{prev} + V_y$. On the other hand, hotspot users choose a random speed between 10 and 20 when they start moving towards their assigned pico cell on their allocated time slot. When they reach their cell, their velocity drops to a random number between 0 and 2 and they choose a different destination within that cell. When their working times elapse, each user chooses a completely random new destination that can be within or outside the cell. This is a valid assumption since we associate UEs with real people who goes to work at specific times and then remain inside their workplaces for some time, where they move with much lower speeds.

Two pseudocodes that explain the initialization and user movements are shown in Algorithm 1 and Algorithm 2, respectively. Hotspot users run both algorithms as they are. On the other hand, random users do not choose a pico cell in the initialization. Also, in the user movement algorithm, since random users do not have a work time, they skip the conditions related to work time and only check if they reached their destinations.

Algorithm 1 Initialization

- 1: $MyPico \leftarrow$ random pico cell
 - 2: $x\text{-coordinate} \leftarrow$ random within macro cell
 - 3: $y\text{-coordinate} \leftarrow$ random within macro cell
 - 4: $x\text{-destination} \leftarrow$ random within macro cell
 - 5: $y\text{-destination} \leftarrow$ random within macro cell
 - 6: $MySpeed \leftarrow$ random between 10m/slot and 20m/slot
 - 7: $MySpeedX \leftarrow$ projection of the speed on x-coordinate
 - 8: $MySpeedY \leftarrow$ projection of the speed on y-coordinate
-

Algorithm 2 User Movement

- if** work time comes **then**
 - 2: $x\text{-destination} \leftarrow$ random within $MyPico$
 $y\text{-destination} \leftarrow$ random within $MyPico$
 - 4: $MySpeed \leftarrow$ random between 10m/slot and 20m/slot
 $MySpeedX \leftarrow$ projection of the speed on x-coordinate
 - 6: $MySpeedY \leftarrow$ projection of the speed on y-coordinate
 - end if**
 - 8: **if** work time ends **then**
 - $x\text{-destination} \leftarrow$ random within macro cell
 - 10: $y\text{-destination} \leftarrow$ random within macro cell
 $MySpeed \leftarrow$ random between 10m/slot and 20m/slot
 - 12: $MySpeedX \leftarrow$ projection of the speed on x-coordinate
 $MySpeedY \leftarrow$ projection of the speed on y-coordinate
 - 14: **end if**
 - $x\text{-coordinate} \leftarrow x\text{-coordinate} + MySpeedX$
 - 16: $y\text{-coordinate} \leftarrow y\text{-coordinate} + MySpeedY$
 - if** destination reached **then**
 - 18: **if** within work time **then**
 - $x\text{-destination} \leftarrow$ random within $MyPico$
 - 20: $y\text{-destination} \leftarrow$ random within $MyPico$
 $MySpeed \leftarrow$ random between 0m/slot and 2m/slot
 - 22: $MySpeedX \leftarrow$ projection of the speed on x-coordinate
 $MySpeedY \leftarrow$ projection of the speed on y-coordinate
 - 24: **else**
 - $x\text{-destination} \leftarrow$ random within macro cell
 - 26: $y\text{-destination} \leftarrow$ random within macro cell
 $MySpeed \leftarrow$ random between 10m/slot and 20m/slot
 - 28: $MySpeedX \leftarrow$ projection of the speed on x-coordinate
 $MySpeedY \leftarrow$ projection of the speed on y-coordinate
 - 30: **end if**
 - end if**
-

4.1.4 Activity Model

All users make the decision of being active or idle in each subsequent time slot. All users are active with probability 0.4 when they are connected to macro eNB and are active with probability 0.8, when they are within a pico cell. The idle users transmit no data to the eNB and in return, when turning on an eNB, we only consider active users inside the cell. When the user is active, we assume that it continuously transmits packets throughout that slot.

In the case of MoNet, the users have the same activity model with the corresponding user distribution. In other words, in the case of MoNet with UDC user distribution, the users that are inside pico cells in UDC configuration, are again active with probability 0.8. We have made this assumption since the activity model of a user is independent from the location of pico cells. In fact, in reality, the cells are placed in locations where the users are active most. In other words, a user uses the Internet more at work, independent from whether there is a hotspot at work or not.

4.1.5 Channel Model

Channel parameters such as path loss formulas and shadow fading standard deviations are obtained from [32], in addition to parameters such as cell radius, transmit powers, total bandwidth and antenna gains. These parameters are summarized in Table 4.1.

Table 4.1: Power Model Parameters for Different Base Station Types [32]

Parameters	Settings/Assumptions
Cell radius	Macro cell: 500m Small cell: 50m
Transmit power	Macro eNB: 46dBm Small cell: 30dBm
Bandwidth	$2 \times 10\text{MHz}$ @ 2GHz and 3.5GHz
Antenna configuration	2×2 MIMO with rank adaptation and interference rejection
Antenna gain	Macro: 14dBi Small cell: 5dBi
Path loss	Macro cell: $140.7 + 36.7 \log_{10}(R[\text{km}])$ Small cell: $128.1 + 37.6 \log_{10}(R[\text{km}])$
Shadow fading	Macro cell: lognormal, std=8dB Small cell: lognormal, std=10dB

4.1.6 Energy Model

In the simulations, one day corresponds to 1000 slots. There are 3 different work times for hotspot users that begin in 0th, 42nd and 83rd slots. The users remain at work for 375 slots, that corresponds to 9 hours. When the number of users within a pico cell exceeds the turn on threshold, the pico eNB first enters a boot mode that lasts for 1 slot and then turns on. The energy consumption parameters that are used in simulations are decided with the help of [27] and [32]. Table 2.1 summarizes the parameters in [27] and Table 4.2 shows the parameters of [32]. We took the values that they both agree on, which means $P_{sleep} = 8.6W$, $P_0 = 13.6W$, $P_{max} = 0.25W$ and $\Delta_p = 4$. The formula that is used to calculate the consumed power is expressed in Equation (2.6). For the boot mode, we assumed that the eNB consumes P_{sleep} and it cannot serve any users for that slot.

Table 4.2: Energy Consumption Parameters for Various Base Station Types [32]

BS type	N_{sec}	P_{max} [W]	P_{max} [dBm]	P_0 [W]	Δ_p	P_{sleep} [W]
Macro	3	40.0	46	260	4.75	150
RRH	3	40	46	168.0	2.8	112.0
	1	5.0	37	103.0	6.5	69.0
	1	1.0	30	96.2	1.5	62.0
	1	0.25	24	13.6	4.0	8.6
Pico	1	5.0	37	103.0	6.5	69
	1	1.0	30	96.2	1.5	62.0
	1	0.25	24	13.6	4.0	8.6
Femto	1	0.1	20	9.6	8.0	5.8

Even though $P_{sleep} = 8.6W$ in Table 4.2, we have also simulated the case where P_{sleep} takes smaller values. That is because, when the eNBs do not serve users for some time, they have a chance to enter a deeper sleep mode and in that case $P_{sleep} = 8.6W$ is a high value. However, there is not much numerical information regarding different sleep mode energy consumption parameters in the literature; thus, we have compared several cases with various P_{sleep} values.

Our regular sleep mode is small cell controlled sleep mode and the deeper sleep mode can be assumed as core network controlled sleep mode. That way, in the deeper sleep mode, since the pico eNB do not require sniffing constantly, it consumes less power.

4.2 Simulation Results

4.2.1 Simulations without Activity Management

In our first network model, transmission energies of eNBs are determined only according to path loss and path loss is determined according to Free Space Model, where the parameters are obtained from [5] and explained in Table 4.3.

Table 4.3: Initial Simulation Parameters [5]

Simulation Parameter	Small cell	Macro cell
Transmit power (P_{max})	1W	1W
Cell radius (R)	50m	500m
Path loss exponent (α)	1.8	2
Additional path loss exponent (β)	1.8	2
BS antenna height (h_{BS})	12.5m	25m
Mobile antenna height (h_{MU})	2m	2m
Receiver sensitivity	-31dBm	-31dBm
Breakpoint distance (g)	300m	600m
System bandwidth (W)	20MHz	
Path loss constant (K)	1	

In the first simulation, we have compared the total energy consumptions of MoNet, COE and UDC with respect to number of users and obtained Figure 4.2. Here, we have assumed that all users have uniformly distributed fixed locations.

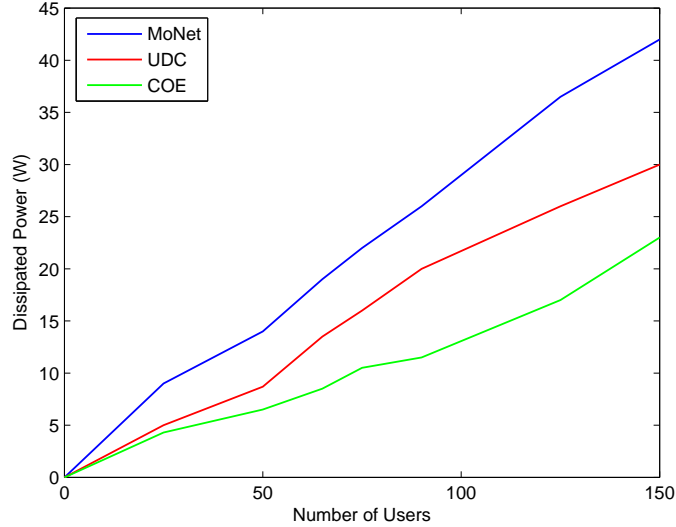


Figure 4.2: Dissipated Power vs. Number of Users

As seen from Figure 4.2, dissipated power increases with increasing number of users, since the total transmission energy is the sum of energies required to communicate with each user. In the simulations without activity management, the fixed power consumption of the base stations is omitted, i.e., $P_0 = 0$. Here, we observe that MoNet performs worst, since the path loss that users face in that topology is much larger than other cases and transmission energies are determined according to path loss. Also, we notice that COE performs better than UDC; since in COE, the users that would face largest path loss are served by the pico eNB, that is located at a smaller distance. That way, the path loss is significantly reduced.

We now assume that the users are mobile and the system is switched to a slotted one. The simulation is rerun for the users with different maximum speeds and the speed of each user in a slot is chosen randomly between 0 and the maximum speed. The resulting graphs are shown in Figure 4.3, Figure 4.4, Figure 4.5, and Figure 4.6. Again, the initial locations of the users are distributed uniformly.

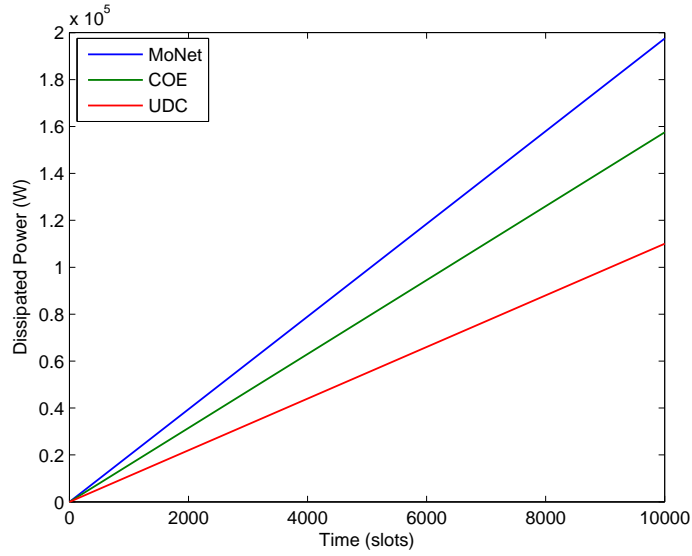


Figure 4.3: Dissipated Power vs. Time for 150 Stationary Users

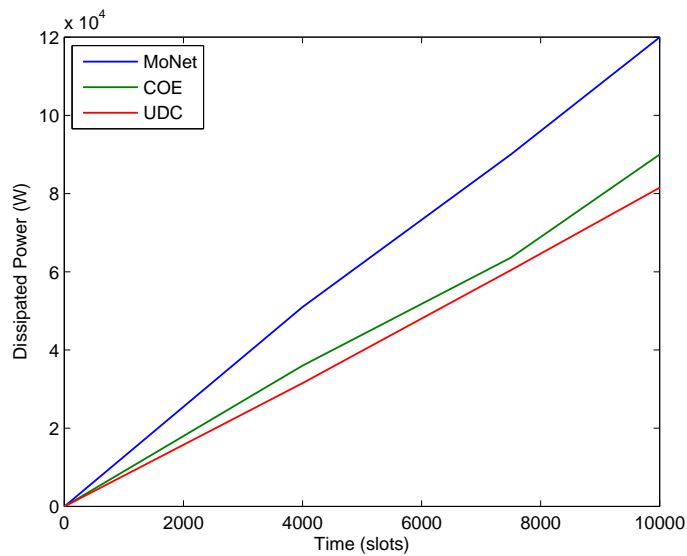


Figure 4.4: Dissipated Power vs. Time for 150 Users with a Maximum Speed of 5 m/slot

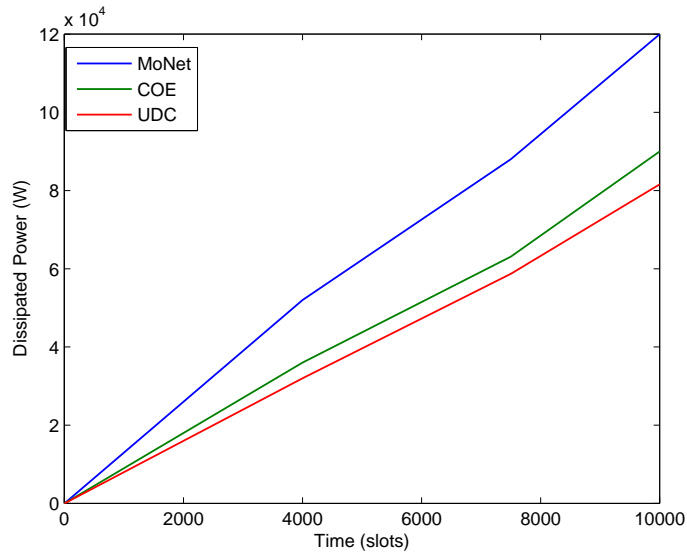


Figure 4.5: Dissipated Power vs. Time for 150 Users with a Maximum Speed of 10 m/slot

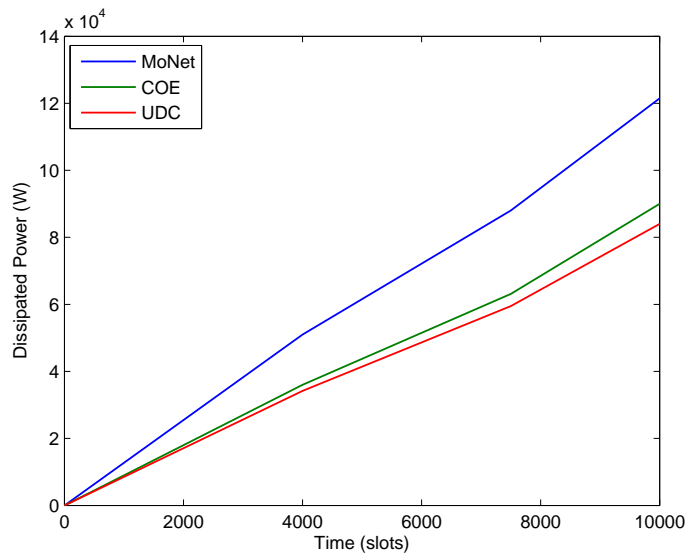


Figure 4.6: Dissipated Power vs. Time for 150 Users with a Maximum Speed of 20 m/slot

These graphs show the dissipated power with respect to time for 150 users. In the case of mobile users, UDC performed better than COE. That is because, in case of stationary users, the maximum energy gain is achieved when the users which are furthest from the macro eNB use pico eNBs; since the transmit energy is determined according to Free Space Model. However, in case of mobile users, since it is less likely for a user to travel on the edges of the simulation area than to travel near the centre, pico cells are less utilized in COE case. Thus, the energy gain for that case is less than UDC.

4.2.2 Simulations with Activity Management

Then, we have changed the energy model to the model explained in Section 4.1.6. After that, dissipated powers of different base stations are calculated using Equation (2.6) and are given as

$$P_{macro} = 780 + \frac{120 \times 4.75 \times n_{user}}{1000} \quad (4.1)$$

$$P_{pico} = 13.6 + \frac{0.25 \times 4 \times n_{user}}{50} \quad (4.2)$$

where the maximum user capacities of macro and pico eNBs are assumed to be 1000 and 50, respectively. We need to assign some values to these parameters, since in Equation (2.6), P_{out} is a fraction of P_{max} , which depends on the ratio of number of users served and the maximum number of users.

When we have changed the energy model, as the fixed energies of eNBs are larger than or comparable to their transmission energies, MoNet has become more efficient than COE and UDC in terms of total consumed power.

4.2.2.1 Single Time-Slot Case

4.2.2.1.1 Uniform User Distribution

In the next simulation, we have assumed that the nodes in sleep mode consume no energy. Again, the users are distributed uniformly and they are assumed to be

active with probability 1. Here, all the pico eNBs are in the sleep mode initially. In this simulation, we consider 100 realizations of one time slot. If the number of users they serve is larger than the threshold in that slot, the nodes switch to active mode. EE, capacity and total dissipated power values for three different turn-on thresholds are inspected in Table 4.4.

Table 4.4: EE, Bit Rate and Dissipated Energy Values for Various Thresholds (T_a)

	Topology	EE (Bits/J)	Bit Rate (Bits/slot)	Energy (J)
$T_a = 0$	MoNet	340,577	4.5977×10^8	1350.00
	COE	325,110	5.0493×10^8	1553.12
	UDC	314,784	4.9512×10^8	1572.91
$T_a = 8$	MoNet	339,764	4.5868×10^8	1350.00
	COE	335,670	4.9476×10^8	1473.96
	UDC	322,315	4.8694×10^8	1510.77
$T_a = 13$	MoNet	339,948	4.5892×10^8	1350.00
	COE	342,915	4.7430×10^8	1383.15
	UDC	342,026	4.6691×10^8	1365.15

As seen from Table 4.4, as we increase the threshold, total capacity decreases; since the number of users being served by pico eNBs lessens. However, when we turn off underutilized cells, we begin to outperform MoNet, in terms of EE. That is because, even though we turn off some cells, we still serve some users within active pico cells and that provides a gain due to path loss. We also get rid of the zero-load powers of underutilized cells.

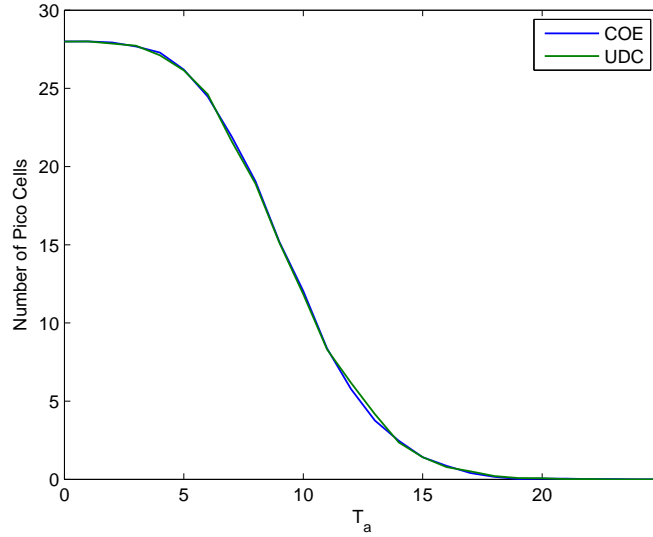


Figure 4.7: Number of Active Pico eNBs vs. T_a

Then, we have rerun the simulation to find the optimum threshold value. Again, we consider 100 realizations of one time slot. The number of active pico cells for different thresholds are as seen from Figure 4.7. When T_a exceeds 18, there are no more active pico cells. This is expected, since the users are uniformly distributed.

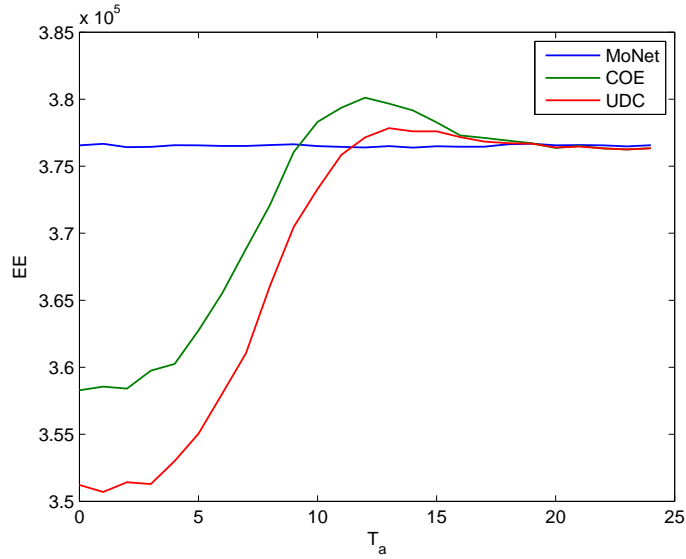


Figure 4.8: EE vs. T_a for MoNet, UDC and COE with $P_{sleep} = 0W$

The change in the EE with respect to threshold can be seen in Figure 4.8. As seen here, the optimum value for T_a is 12 for COE and 13 for UDC. Also, COE performs better than UDC, since here, we only see the effect of path loss but not mobility, as we only consider 1 time slot.

Then, to see the effect of pico cells more, on top of the EE graph of COE, UDC and MoNet, we have added COE and UDC without the energy and bit rate of macro cell. The resulting graph is shown in Figure 4.9.

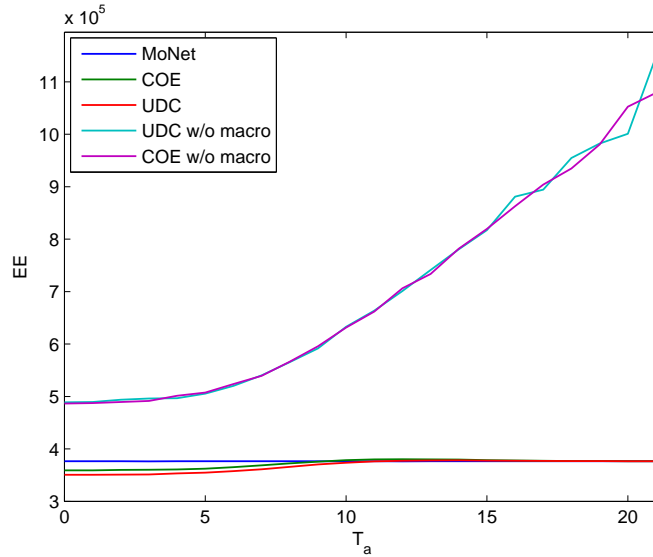


Figure 4.9: EE vs. T_a for MoNet, UDC, COE, UDC w/o Macro and COE w/o Macro with $P_{sleep} = 0W$

As seen from the figure, EE of the users of pico cells are considerably large. However, the number of users in pico cells is very small. So, the benefit of using pico cells from the overall EE of the entire HetNet is not visible in the case of uniform user distribution.

However, these results are for $P_{sleep} = 0W$, as expressed before. When we take $P_{sleep} = 8.6W$, which is the value provided in [25], Figures 4.8 and 4.9 transform into Figures 4.10 and 4.11, respectively.

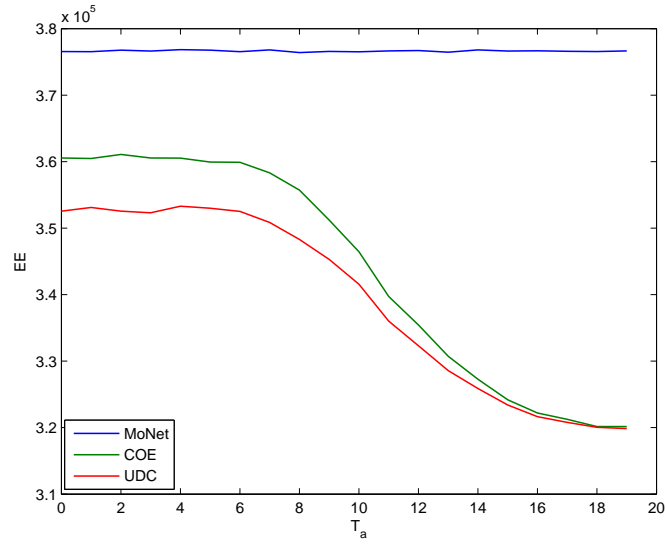


Figure 4.10: EE vs. T_a for MoNet, UDC and COE with $P_{sleep} = 8.6W$

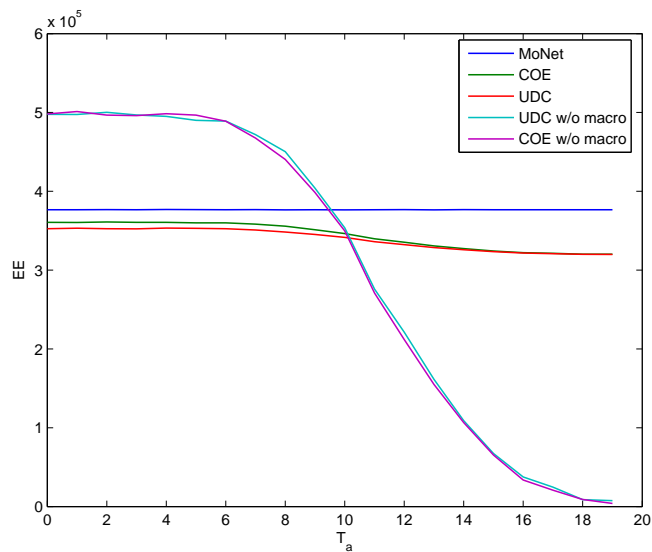


Figure 4.11: EE vs. T_a for MoNet, UDC, COE, UDC w/o Macro and COE w/o Macro with $P_{sleep} = 8.6W$

As seen from Figures 4.10 and 4.11, since the sleep energies of the nodes are quite high, when we turn off underutilized nodes, their large sleep energies cause a significant decrease in overall EE. In order to increase the overall network EE, we should either implement a sleep mode with a smaller sleep energy or increase the number of users within pico cells.

In addition, to see the fairness between users in terms of bit rates, the histogram of bit rates have been drawn for $T_a = 2$, $T_a = 8$ and $T_a = 12$. Once again, we consider 100 realizations of one time slot. The histograms of users in MoNet, COE and UDC are as as shown in Figures 4.12, 4.13 and 4.14, respectively.

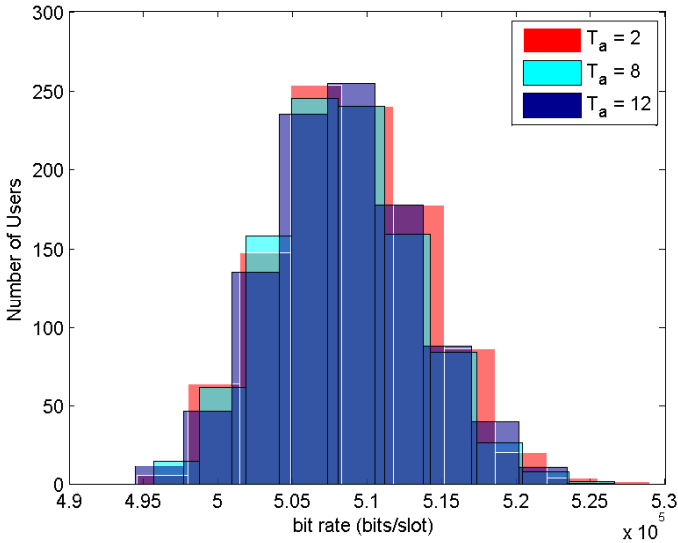


Figure 4.12: Histogram of bit rates achieved by MoNet users for $T_a = 2$, 8 and 12

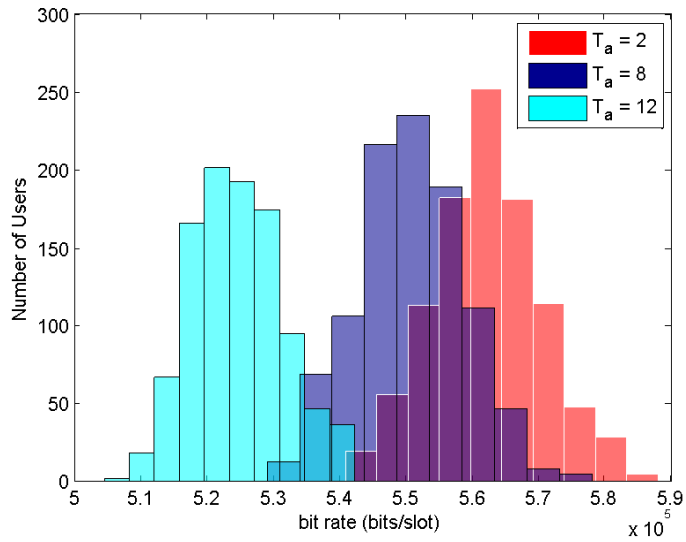


Figure 4.13: Histogram of bit rates achieved by COE users for $T_a = 2, 8$ and 12

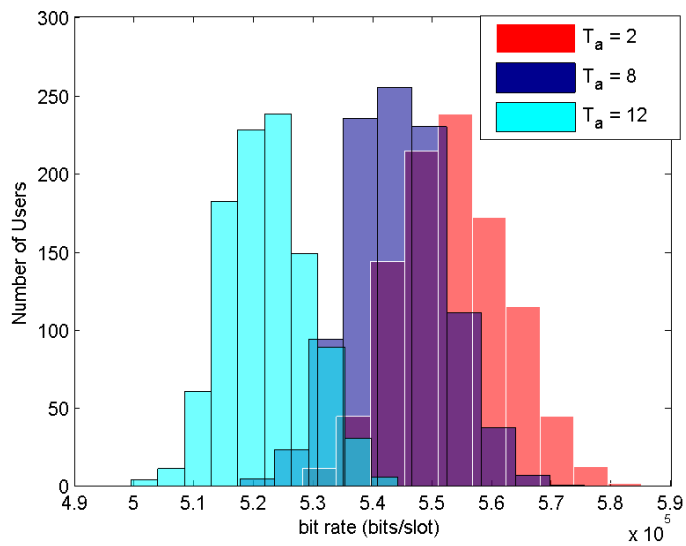


Figure 4.14: Histogram of bit rates achieved by UDC users for $T_a = 2, 8$ and 12

In MoNet, the change in the thresholds do not change the histogram of capacities, since there are no pico eNBs to turn on and off. But in UDC and COE, as the threshold increases, users get less capacities as expected, since fewer number of users are able to use pico cells, when T_a is large. For instance, when $T_a = 2$ and most pico cells are active, some users in COE and UDC get a capacity around 5.9×10^5 b/s. Also, on the average, they get around 5.6×10^5 b/s. When $T_a = 12$, the highest capacity that the users get becomes 5.45×10^5 b/s and the average capacity becomes 5.25×10^5 b/s. These values are very close to MoNet case, since when T_a is high, most pico eNBs are turned off.

4.2.2.1.2 Hotspot User Distribution

In the next simulations, we use the hotspot model and compared the EE of MoNet, COE and UDC users, varying sleep energies and number of users in hotspots (N_h). While varying the sleep energies of eNBs, we have assumed N_h to be 500; and while varying N_h , we have considered two sleep energies: $P_{sleep} = 0$ and $P_{sleep} = 8.6$. In these simulations, again we have considered 100 realizations of one time slot. Figures 4.15, 4.16, 4.17, 4.18 and 4.19 show the performances of different topologies as T_a changes for various sleep energies.

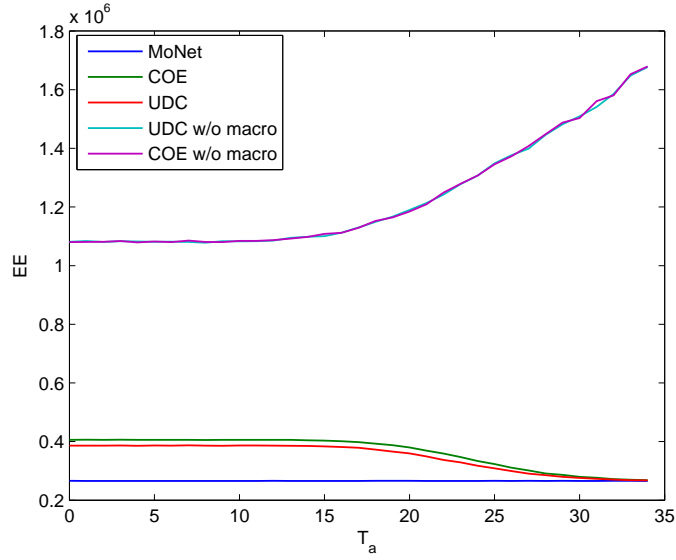


Figure 4.15: EE vs. T_a for MoNet, UDC, COE, UDC w/o Macro and COE w/o Macro with $P_{sleep} = 0W$ and $N_h = 500$

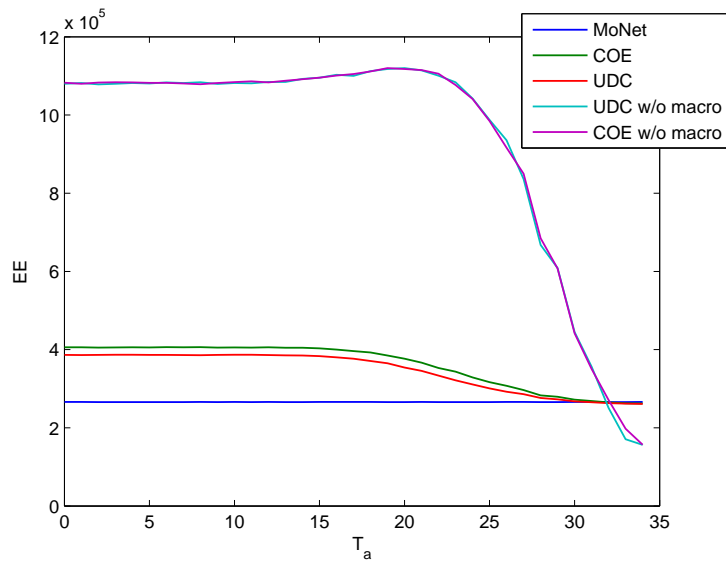


Figure 4.16: EE vs. T_a for MoNet, UDC, COE, UDC w/o Macro and COE w/o Macro with $P_{sleep} = 2W$ and $N_h = 500$

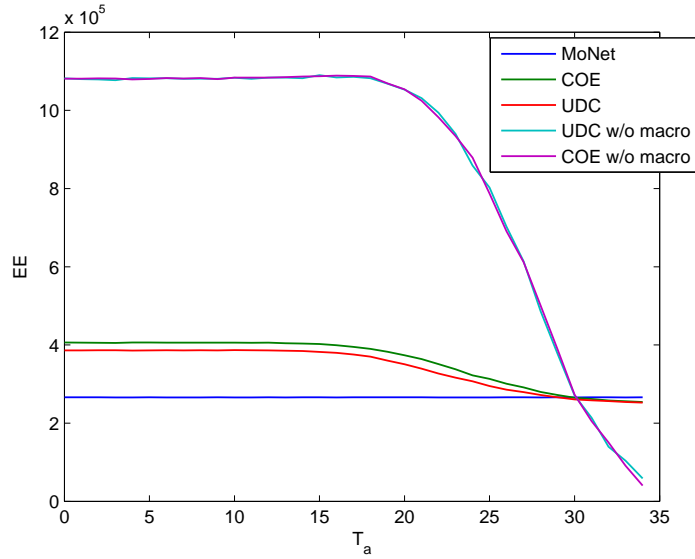


Figure 4.17: EE vs. T_a for MoNet, UDC, COE, UDC w/o Macro and COE w/o Macro with $P_{sleep} = 4W$ and $N_h = 500$

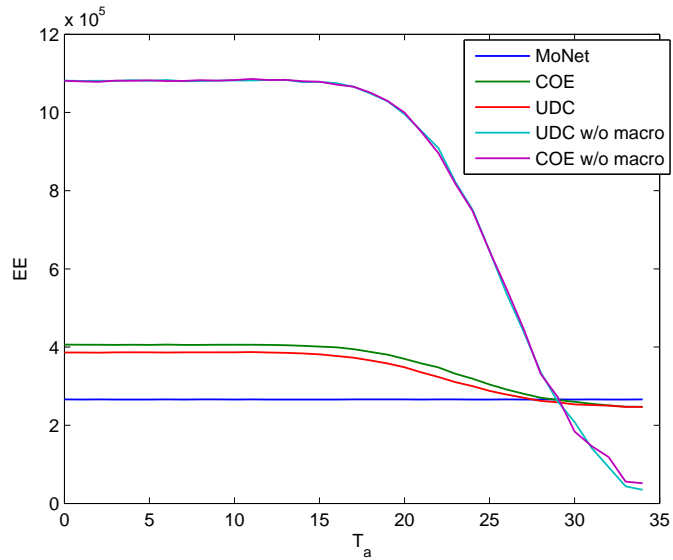


Figure 4.18: EE vs. T_a for MoNet, UDC, COE, UDC w/o Macro and COE w/o Macro with $P_{sleep} = 6W$ and $N_h = 500$

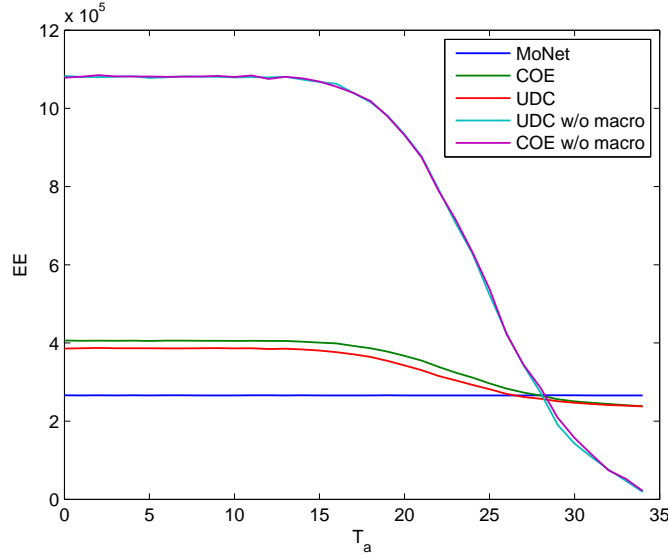


Figure 4.19: EE vs. T_a for MoNet, UDC, COE, UDC w/o Macro and COE w/o Macro with $P_{sleep} = 8.6W$ and $N_h = 500$

As we see from the figures, as the sleep energies of pico eNBs increase, EE of COE and UDC users start to drop below the EE of MoNet users, for large values of T_a . That is because, when $T_a < 15$, no pico eNB is in the sleep mode; thus sleep energies of pico eNBs do not affect the performance. However, when $T_a > 25$, many of the pico cells begin to turn off and consume sleep energy. As a result, when most or all of them are turned off, the users begin to be served by macro cell, but pico eNBs consume additional sleep energies. Then, the EE of COE and UDC users drop below the EE of MoNet users.

Then, we have investigated the effect of number of hotspot users on the network performance in terms of EE. First, we have taken $P_{sleep} = 0W$, and varied the number of hotspot users from 0 to 750. We have already given the results of the cases where $N_h = 0$ and $N_h = 500$ in Figures 4.9 and 4.15, respectively. The resulting graphs of the cases where $N_h = 250$ and $N_h = 750$ are shown in Figures 4.20 and 4.21, respectively.

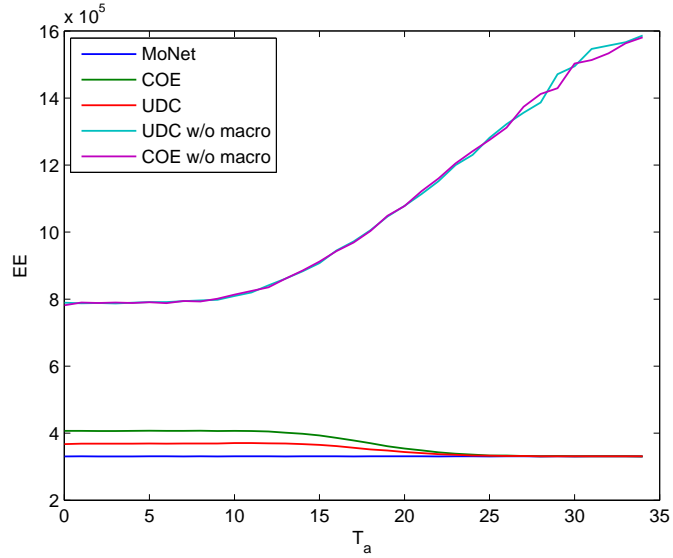


Figure 4.20: EE vs. T_a for MoNet, UDC, COE, UDC w/o Macro and COE w/o Macro with $P_{sleep} = 0W$ and $N_h = 250$

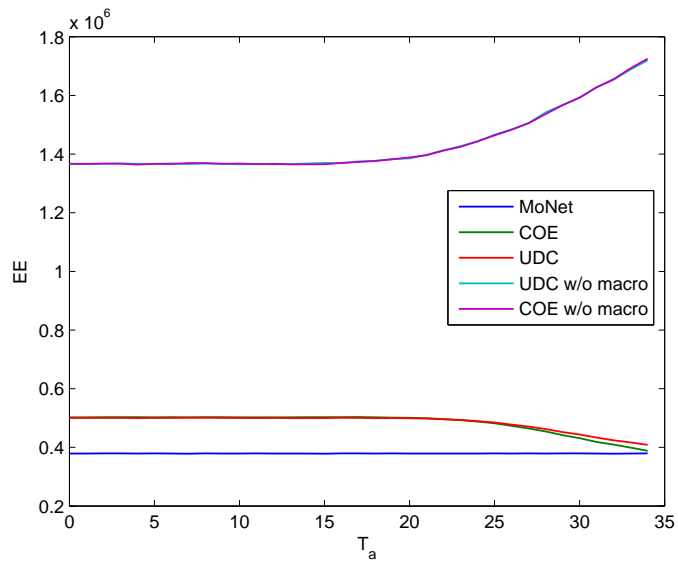


Figure 4.21: EE vs. T_a for MoNet, UDC, COE, UDC w/o Macro and COE w/o Macro with $P_{sleep} = 0W$ and $N_h = 750$

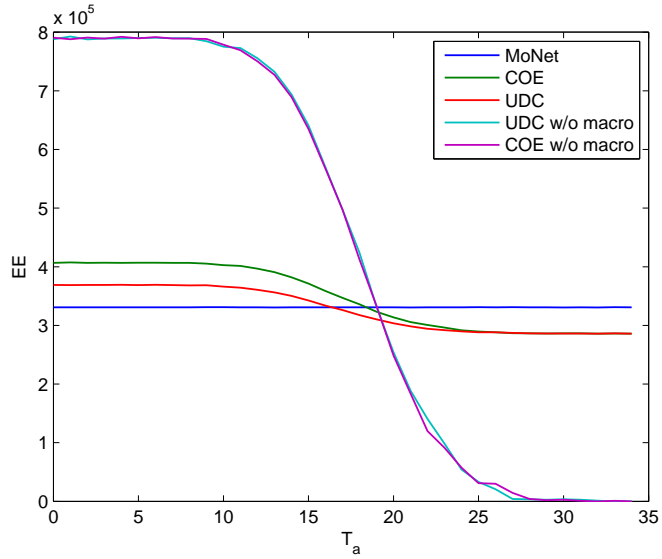


Figure 4.22: EE vs. T_a for MoNet, UDC, COE, UDC w/o Macro and COE w/o Macro with $P_{sleep} = 8.6W$ and $N_h = 250$

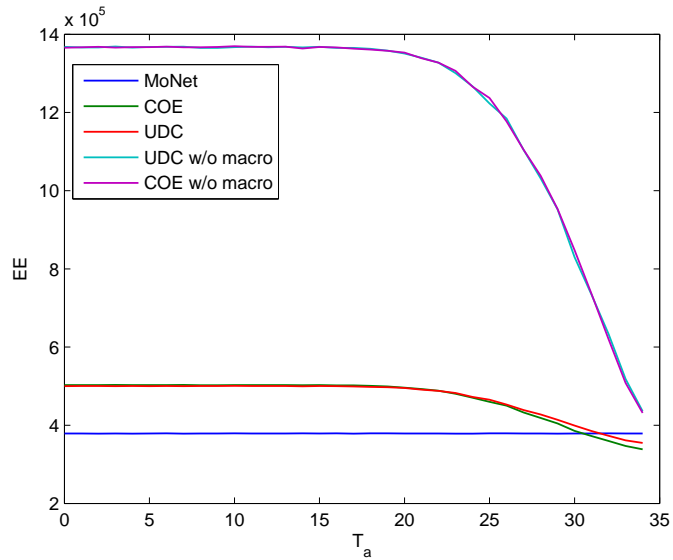


Figure 4.23: EE vs. T_a for MoNet, UDC, COE, UDC w/o Macro and COE w/o Macro with $P_{sleep} = 8.6W$ and $N_h = 750$

After that, we have taken $P_{sleep} = 8.6W$, and varied the number of hotspot users, N_h , from 0 to 750. Again, we have given the results of the cases where $N_h = 0$ and $N_h = 500$ in Figures 4.10 and 4.19. The resulting graphs of the cases where $N_h = 250$ and $N_h = 750$ are shown in Figures 4.22 and 4.23, respectively.

When we compare these figures, we observe that as the number of hotspot users increase, the difference between HetNet scenarios and MoNet increases. Thus, our aim should be increasing the number of hotspot users and decreasing the sleep energies of pico eNBs. We may not change the dissipated power of the nodes in sleep mode; however, we may define a deeper sleep mode with less sleep energy and less features of nodes. Also, we can increase the number of hotspot users by placing the pico eNBs to the areas with higher user density.

We also observe that in the case with hotspot users, the effect of T_a becomes less significant. Because, when there are hotspot users, the more active the pico eNBs are, the more UDC and COE outperforms MoNet. As the pico eNBs start to turn off, EEs of UDC and COE approach to, or even become worse than the EE of MoNet. Thus, in that case, it is better to turn on all the pico eNBs at all times.

In addition, to see the fairness between users in terms of bit rates, the histogram of bit rates have been drawn for $T_a = 5$, $T_a = 21$ and $T_a = 27$, and $N_h = 500$. Once again, we consider 100 realizations of one time slot. The histograms of users in MoNet, COE and UDC are as as shown in Figure 4.24, 4.25 and 4.26, respectively. Here, $P_{sleep} = 8.6W$, but this does not make a difference in the bit rates.

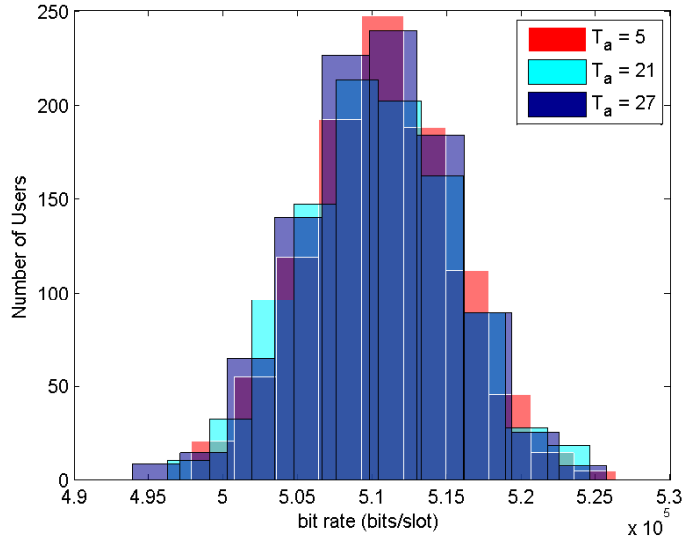


Figure 4.24: Histogram of bit rates achieved by MoNet users for $T_a = 5, 21$ and 27 , and $N_h = 500$

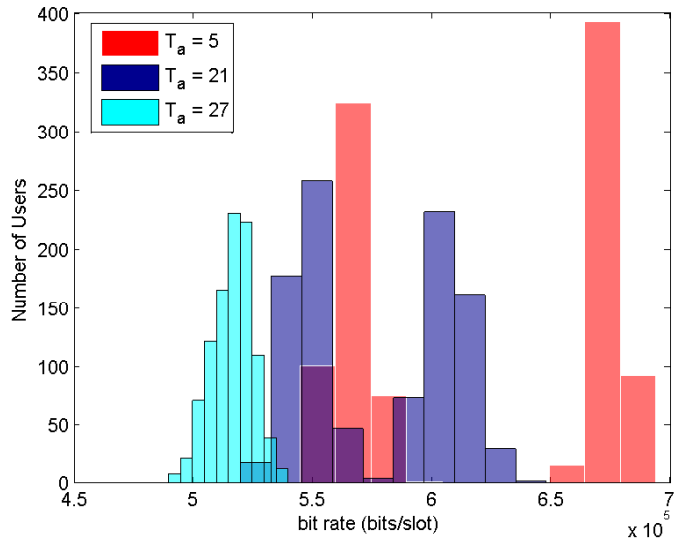


Figure 4.25: Histogram of bit rates achieved by COE Users for $T_a = 5, 21$ and 27 , and $N_h = 500$

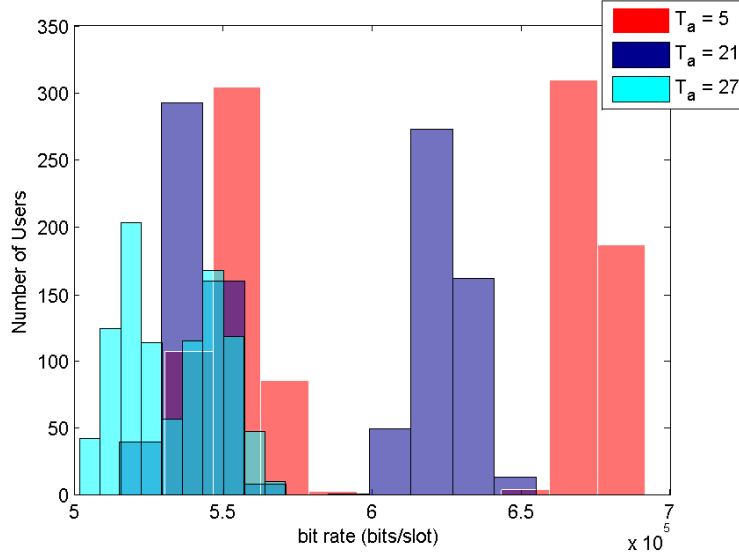


Figure 4.26: Histogram of bit rates achieved by UDC Users for $T_a = 5, 21$ and 27 , and $N_h = 500$

In MoNet, the change in the thresholds do not change the histogram of bit rates, since there are no pico eNBs. But in UDC and COE, as T_a increases, users get less bit rates as expected, since fewer number of users are able to use pico cells, when T_a becomes higher. On the other hand, when T_a is low, the users in UDC and COE achieve noticeably higher bit rates, compared to MoNet. Also, in Figures 4.25 and 4.26, we observe that when $T_a = 5$ or 21 , the histogram is split. This is because, there is a difference between the bit rates of the users that are served by macro and pico eNBs, and when $N_h = 500$, the number of users served by pico eNBs are quite significant. Thus, the bit rates of the users that are served by pico eNBs are considerably larger than the bit rates of the users that are served by macro eNBs. However, when $T_a = 27$, since the number of users served by pico eNBs is very small, the bit rates they get do not appear apart from the other users. This split histograms are the main difference from the histograms in Figures 4.12, 4.13 and 4.14; since in that case, number of pico cell users were much smaller than the hotspot case. In addition, since we take the average of 100 realizations, the maximum bit rates in Figures 4.25 and 4.26 are

higher than that of Figures 4.13 and 4.14, since the probability of a user being within a pico cell is higher in hotspot scenario and users in pico cells get higher bit rates.

4.2.2.2 Multiple Time-Slots Case

In the next simulation, we have compared the performances of the topologies with respect to time. We have run the simulation for 1000 slots, which corresponds to 1 day. As expressed before, users are mobile with a random speed between 10-20 m/slot. There are 500 hotspot and 500 randomly distributed users. Inside a pico cell, hotspot users are active with probability 0.8, and outside they are active with probability 0.4, as well as random users. The working times of hotspot users begin at slots 0, 42 and 83; and then, they begin moving towards their assigned pico cells. The change in the EE with respect to time for $P_{sleep} = 0W$ and $P_{sleep} = 8.6W$ are shown in Figures 4.27 and 4.28, respectively. MoNet with COE configuration and MoNet with UDC configuration are as defined in Section 4.1.2.2.

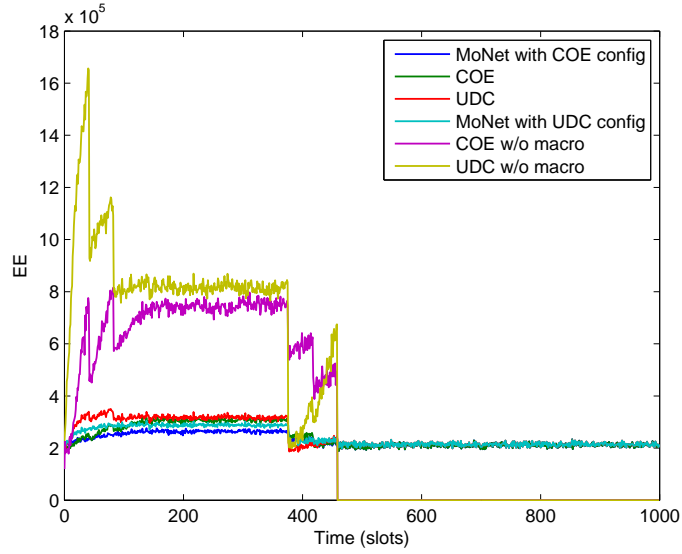


Figure 4.27: EE vs. time for MoNet, UDC, COE, UDC w/o Macro and COE w/o Macro with $P_{sleep} = 0W$ and $N_h = 500$

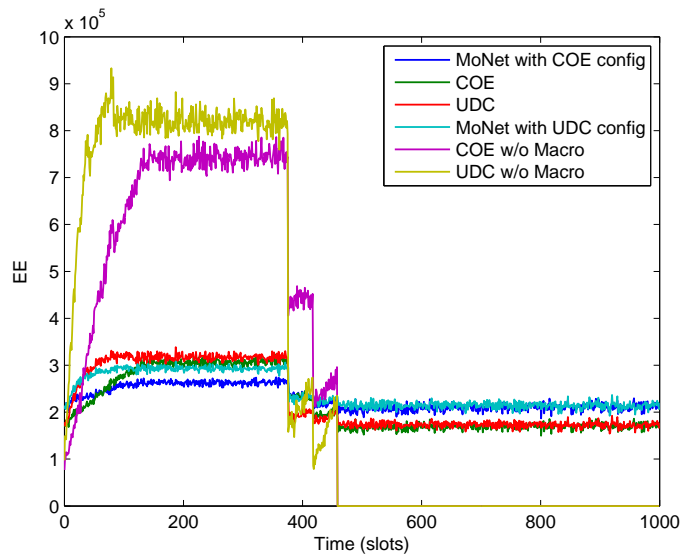


Figure 4.28: EE vs. time for MoNet, UDC, COE, UDC w/o Macro and COE w/o Macro with $P_{sleep} = 8.6W$ and $N_h = 500$

In Figure 4.27, pico cells have no sleep energy; thus, when they turn off, COE and UDC have the same EE with MoNet. However, in Figure 4.28, the sleep energies of the cells are assumed as 8.6W. Thus, when the pico cells turn off, the EE of UDC and COE fall below MoNet.

Since all users do not arrive their pico cells at the same time, the increase in the EE at the beginning is not sharp. On the other hand, during turn off, as the pico cells stop serving users instantly, EE drops right away. Also, the EE of COE reaches its maximum value later than UDC. That is because the pico cells are located at the edges of the simulation area and it takes longer time to reach them.

Here, UDC has higher EE, since both UDC and COE provide approximately the same EE to pico cell users, but random users have a higher probability to be served by UDC. Also, there is around 20% improvement for both cases. To find the improvements, we have compared UDC with MoNet with UDC configuration and COE with MoNet with COE configuration.

Then, we have inspected the number of users served by pico and macro eNBs in UDC and COE. The resulting graphs are shown in Figures 4.29 and 4.30. Here, $N_h = 500$.

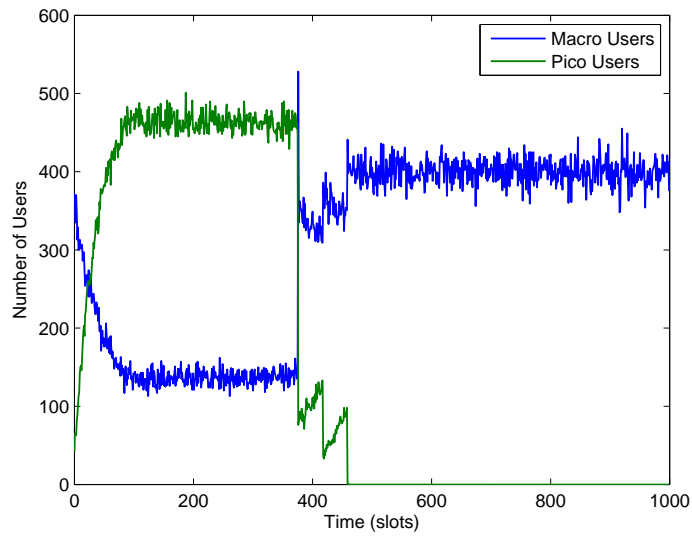


Figure 4.29: Number of Users Served by Pico and Macro Cells vs. Time in UDC

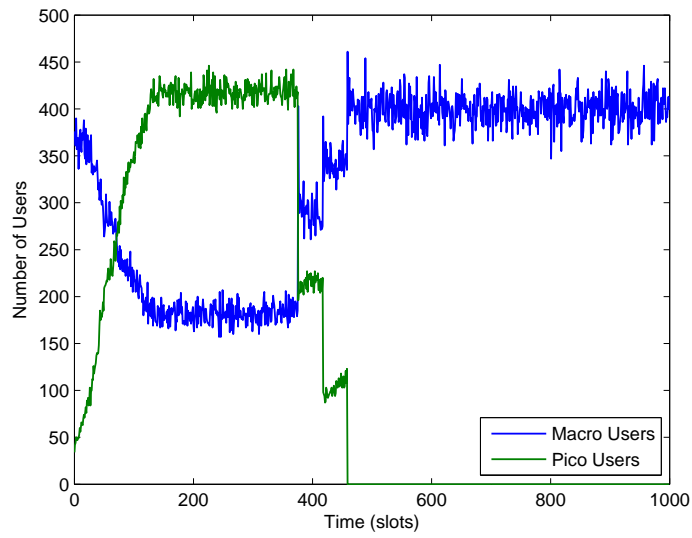


Figure 4.30: Number of Users Served by Pico and Macro Cells vs. Time in COE

In Figure 4.29, we can see the number of active users with respect to time. Number of active macro users start from 400; since, when all the pico cells are turned off, all 1000 users are connected to macro eNB and they are active with probability 0.4. Around 100th slot, all assigned users are inside their pico cells and active with probability 0.8, thus, number of pico users should be at least 400. They are around 470, since some of the randomly distributed users are also within pico cells. Finally, around 470th slot, pico cells are turned off and all 1000 users are connected to macro eNB again. As they are active with probability 0.4, number of active macro users become around 400.

In Figure 4.30, number of active macro users start from 400, too. On the contrary to the UDC, here the assigned users reach their pico cells around 150th slot, since the pico cells are on the edges of the simulation area. Then, the number of active users in pico cells reach around 410. That is because, the number of random users being served by pico eNBs is very low, since they are located at the end of the coverage area of macro cell. When pico eNBs start to turn off, the number of users inside the pico cells do not drop as fast as UDC; since in the case of COE, when a user leaves a pico cell, it is very likely to enter another pico cell, as they are located side by side. And when the user enters the neighbour cell, that cell may not be turned off yet. Thus, the total number of users being served by pico eNBs do not drop as fast as in UDC. Finally, around 470th slot, pico cells are turned off and all 1000 users are connected to macro eNB again. As they are active with probability 0.4, number of active macro users become around 400.

Then, in order to see difference between the one-threshold system and the two-threshold system, we have rerun the simulation for the sleep energies $P_{sleep} = 0W$ and $P_{sleep} = 8.6W$, and various thresholds. When there is only one threshold, we assume that the pico cell turns on when the number of users within the cell is larger than or equal to the threshold; and it turns off when the number of users gets strictly less than the threshold. When there are two thresholds, we assume that the pico cell turns on when the number of users within the cell is larger than or equal to the T_a ; and it turns off when the number of users gets less than or equal to T_d .

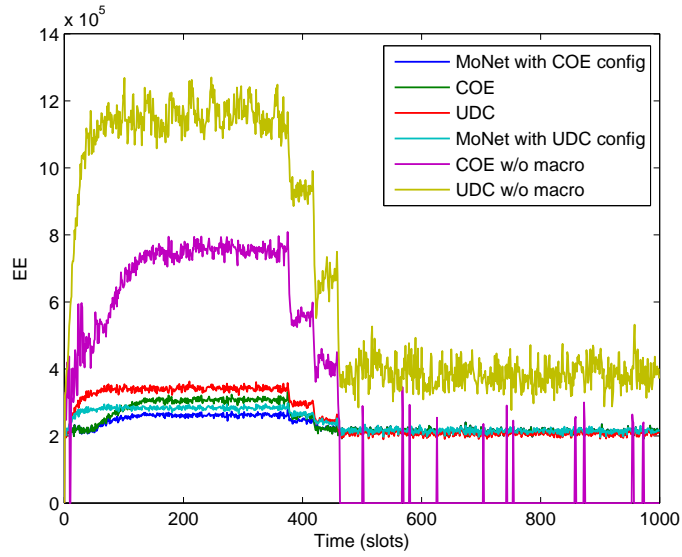


Figure 4.31: EE vs. time for $P_{sleep} = 0W$ and $T_a = 5$

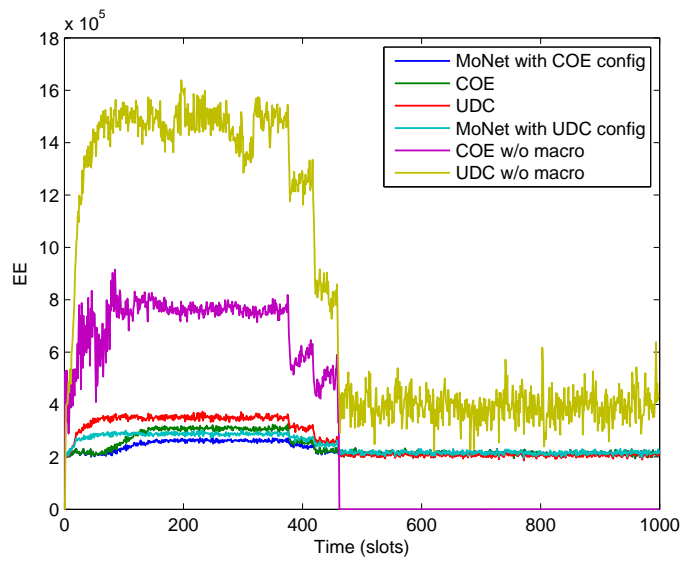


Figure 4.32: EE vs. time for $P_{sleep} = 0W$, $T_a = 9$ and $T_d = 4$

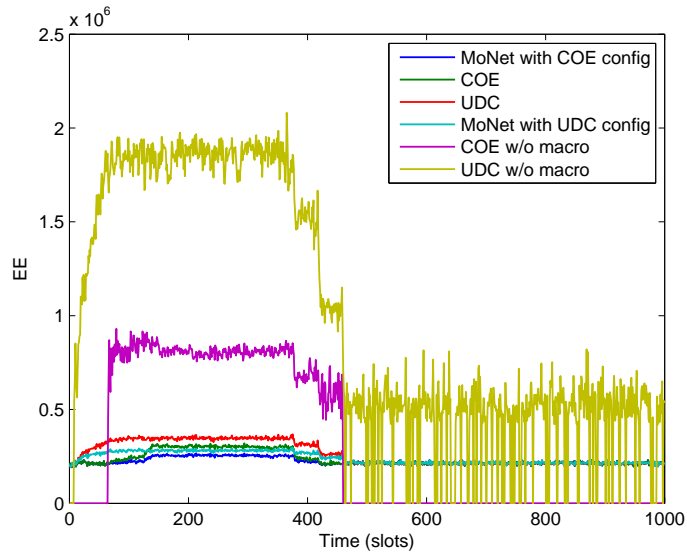


Figure 4.33: EE vs. time for $P_{sleep} = 0W$ and $T_a = 9$

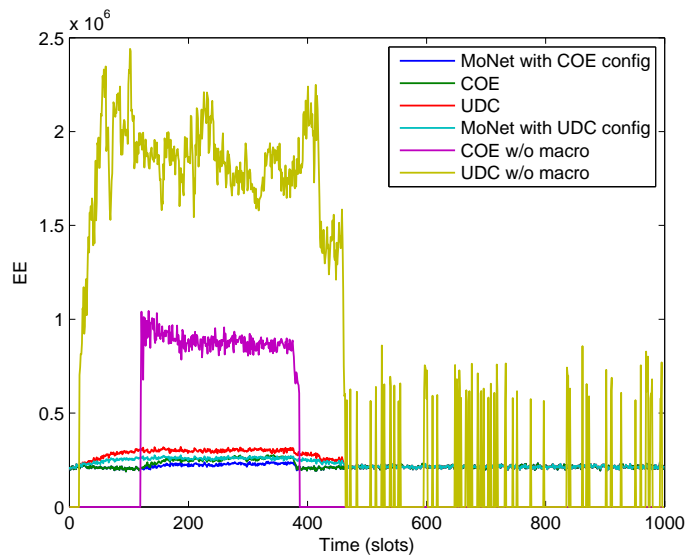


Figure 4.34: EE vs. time for $P_{sleep} = 0W$ and $T_a = 12$

In Figure 4.31, the average improvement in the EE is around 20% and even after 470th slot, some pico eNBs in UDC remain active. However, in COE, pico eNBs seldom turn on after 470th slot. At the same time, in Figure 4.32, again the average improvement in the EE is around 20%. However, this time, the pico eNBs in COE never remain active after 470th slot. In Figure 4.33, once again the average improvement is around 20%. In this case, after 470th slot, some pico eNBs in UDC oscillate between active and sleep modes, as there is only one threshold. But since $P_{sleep} = 0W$, this oscillation does not affect the system performance.

The improvement is around 20% for Figures 4.31, 4.32 and 4.33. This result is expected; since from Figure 4.15, we know that T_a being 5 or 9 does not change the performance of the system. Another observation from Figures 4.31, 4.32 and 4.33 is that the location of T_a does not affect the system, since between slots 0 and 470, the number of users in pico cells is quite large and the probability of oscillation is almost 0. After 470th slot, even though an oscillation occurs, as $P_{sleep} = 0W$, this oscillation does not affect the system performance. On the other hand, in Figure 4.34, the average improvement in the EE is less than 20%, since not all the pico cells are able to turn on, when $T_a = 12$. Thus, even though the location of the second threshold does not affect the system performance much, T_a should be chosen in a way to maximize active pico cells, i.e., it should not be very large.

When $P_{sleep} = 8.6W$, the previous graphs transform into Figures 4.35, 4.36, 4.37 and 4.38.

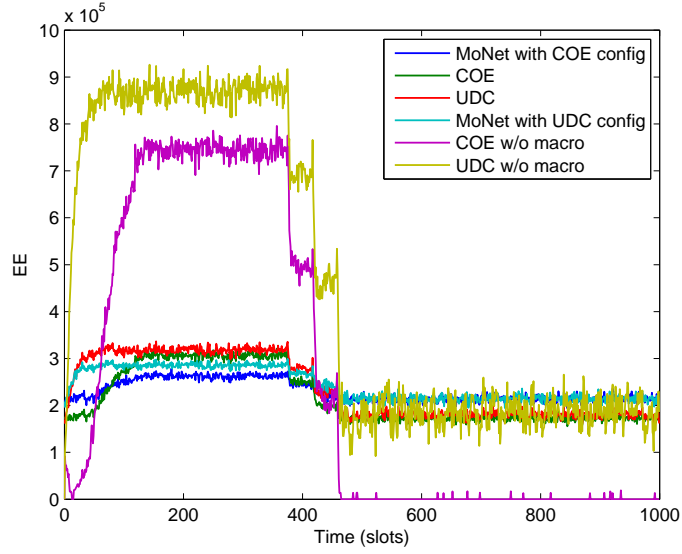


Figure 4.35: EE vs. time for $P_{sleep} = 8.6W$ and $T_a = 5$

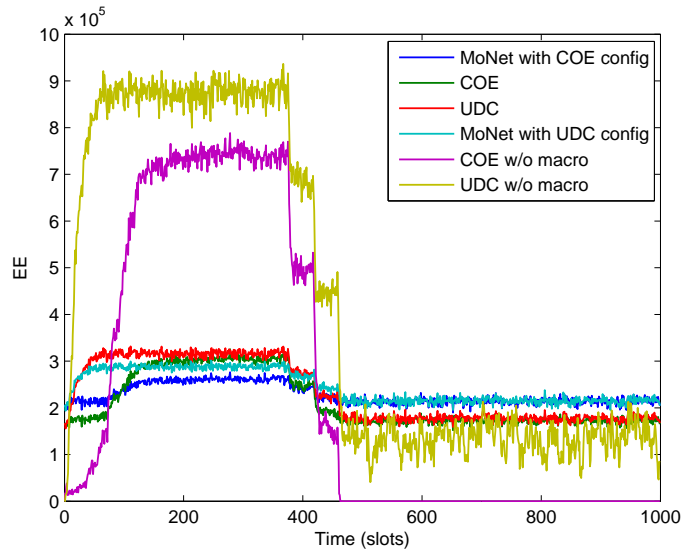


Figure 4.36: EE vs. time for $P_{sleep} = 8.6W$, $T_a = 9$ and $T_d = 4$

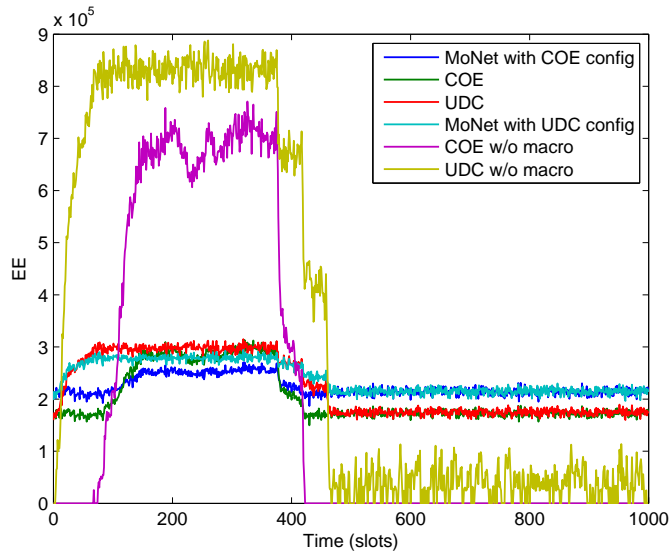


Figure 4.37: EE vs. time for $P_{sleep} = 8.6W$ and $T_a = 9$

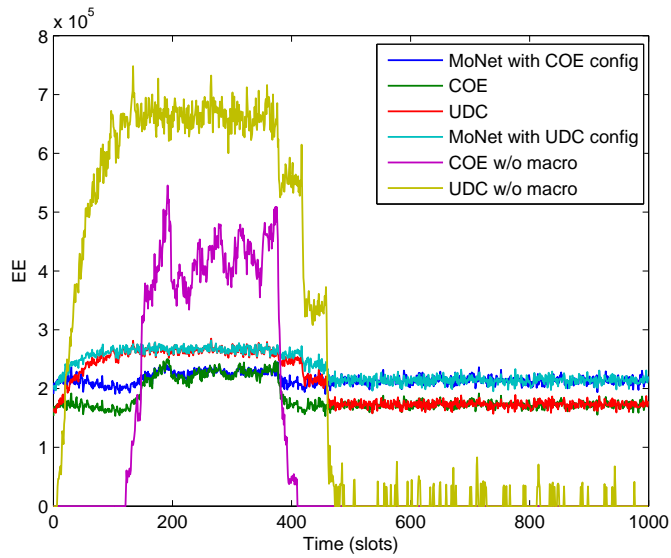


Figure 4.38: EE vs. time for $P_{sleep} = 8.6W$ and $T_a = 12$

In Figures 4.35, 4.36 and 4.37, average improvement in the EE between slots 0 and 470 is around 20%, which is the same as before. This is expected since all pico eNBs are active in that interval; thus, the value of P_{sleep} does not affect the performance of the system between those slots. However, when we compare Figures 4.36 and 4.37, we observe that T_d becomes important in the case where $P_{sleep} = 8.6W$. Because, it is more beneficial for the system when more pico cells remain active after 470th slot. Thus, we want T_d to be as low as possible. We also observe that the performances of COE and UDC are lower than MoNet, after 470th slot. This is because most pico cells are in sleep mode after that slot; thus, in addition to not providing capacity to the system, they consume sleep energy.

Also, when we investigate Figure 4.38, we see that there is no improvement between slots 0 and 470. In addition, after 470th slot, the performance of COE and UDC is worst among all simulations, since almost all pico cells are in sleep mode, both in UDC and COE. In short, in the case of hotspot users, both T_a and T_d should be chosen as small as possible, e.g. $T_a = T_d = 0$, since the system benefits most when most pico cells are active.

Chapter 5

Conclusion

In this thesis, a smart sleep strategy for small cell base stations is proposed for improving the energy efficiency of HetNets. When the number of users within the coverage area of an inactive small cell base station exceeds the activation threshold, T_a , the base station is switched to the active mode. On the other hand, when the number of users within the coverage area of an active small cell base station drops below the deactivation threshold, T_d , the base station is turned off.

When the users have uniformly distributed initial locations and $P_{sleep} = 0$ for pico eNBs, the choice of T_a is critical. However, when $P_{sleep} > 0$, there is a penalty for turning off an eNB and EE decreases monotonically with T_a . Thus, it is more beneficial for all pico eNBs that have at least one user to be active. In the case of hotspot users, EE vs. threshold graphs are again monotonically decreasing, so again, turning on all pico eNBs is more efficient.

On the other hand, when the users' motions are not random, i.e., they move according to a hotspot model so as to enter and leave pico cells in groups, HetNet becomes more beneficial. Because, in that model, the number of users per pico cell increases and in return, the effect of offset power of the base station decreases. In the case of hotspot users, the bit rate provided by HetNet can get as high as 6.8×10^5 b/s, which is an increase by 29%, compared to MoNet. Meanwhile, the

energy efficiency increases by 20%.

In short, using the proposed activity control algorithm, we are able to increase the average bit rate of the users while consuming the energy more efficiently. Since, we have simulated various networking scenarios with different topologies, sleep energies and user distributions, we have been able to analyse the effects of several parameters on the network performance.

Future research may be directed to consideration of cooperative strategies for activity control of small cell base stations where joint consideration of number of users in neighbouring small cells is employed. That way, the users within the coverage of inactive small cell base stations can be served by nearby active small cell base stations to increase spectral efficiency.

Bibliography

- [1] M. Harris, “Think small: micro, pico and femto cell sites.” <http://www.unisonsite.com/resource-center/resource.html?article=23>, 2011. Accessed: 2014-06-17.
- [2] V. Pauli, J. D. Naranjo, and E. Seidel, “Heterogeneous LTE networks and inter-cell interference coordination,” *Nomor Research GmBH*, 2010.
- [3] S. Anand, “Heterogeneous networks motivation, types, and techniques used.” http://lteuniversity.com/get_trained/expert_opinion1/b/sekhar/archive/2013/10/02/heterogeneous-networks-motivation-types-and-techniques-used.aspx, 2013. Accessed: 2014-04-12.
- [4] M. Gruber, O. Blume, D. Ferling, D. Zeller, M. A. Imran, and E. C. Strinati, “EARTH energy aware radio and network technologies,” in *IEEE 20th International Symposium on Personal, Indoor and Mobile Radio Communications*, pp. 1–5, IEEE, 2009.
- [5] M. Z. Shakir, K. A. Qaraqe, H. Tabassum, M.-S. Alouini, E. Serpedin, and M. A. Imran, “Green heterogeneous small-cell networks: toward reducing the CO2 emissions of mobile communications industry using uplink power adaptation,” *IEEE Communications Magazine*, vol. 51, no. 6, 2013.
- [6] Y. S. Soh, T. Q. Quek, M. Kountouris, and H. Shin, “Energy efficient heterogeneous cellular networks,” *IEEE Journal on Selected Areas in Communications*, vol. 31, no. 5, pp. 840–850, 2013.

- [7] X. Zhang, Z. Su, Z. Yan, and W. Wang, "Energy-efficiency study for two-tier heterogeneous networks (HetNet) under coverage performance constraints," *Mobile Networks and Applications*, vol. 18, no. 4, pp. 567–577, 2013.
- [8] O. Blume, H. Eckhardt, S. Klein, E. Kuehn, and W. M. Wajda, "Energy savings in mobile networks based on adaptation to traffic statistics," *Bell Labs Technical Journal*, vol. 15, no. 2, pp. 77–94, 2010.
- [9] I. Ashraf, F. Boccardi, and L. Ho, "Sleep mode techniques for small cell deployments," *Communications Magazine, IEEE*, vol. 49, no. 8, pp. 72–79, 2011.
- [10] L. Falconetti, P. Frenger, H. Kallin, and T. Rimhagen, "Energy efficiency in heterogeneous networks," in *Online Conference on Green Communications (GreenCom), 2012 IEEE*, pp. 98–103, IEEE, 2012.
- [11] W. Tranter, K. Shanmugan, T. Rappaport, and K. Kosbar, *Principles of communication systems simulation with wireless applications*. Prentice Hall Press, 2003.
- [12] D. Tse, *Fundamentals of wireless communication*. Cambridge University Press, 2005.
- [13] A. Goldsmith, *Wireless communications*. Cambridge University Press, 2005.
- [14] A. M. Mousa, "Prospective of fifth generation mobile communications," *International Journal of Next-Generation Networks*, vol. 4, no. 3, 2012.
- [15] C. K. Toh, *Ad hoc mobile wireless networks: protocols and systems*. Pearson Education, 2001.
- [16] P. Sharma, "Evolution of mobile wireless communication networks-1G to 5G as well as future prospective of next generation communication network," *International Journal of Computer Science and Mobile Computing*, vol. 2, no. 8, pp. 47–53, 2013.
- [17] J. Parikh and A. Basu, "LTE Advanced: The 4G mobile broadband technology," *IEEE Spectrum*, vol. 5, no. 2.5, p. 30, 2011.

- [18] “3GPP TR 36.814 further advancements for E-UTRA physical layer aspects (release 9).” <http://www.3gpp.org/DynaReport/36814.htm>, 2010. Accessed: 2014-04-17.
- [19] J.-P. M. Linnartz, *Wireless Communication: The Interactive Multimedia CD-ROM*. Baltzer Science Publishers, 2001.
- [20] M. Peuhkuri, “Ip quality of service,” *Helsinki University of Technology, Laboratory of Telecommunications Technology*, pp. 2–0, 1999.
- [21] F. Héliot, O. Onireti, and M. A. Imran, “An accurate closed-form approximation of the energy efficiency-spectral efficiency trade-off over the MIMO rayleigh fading channel,” in *IEEE International Conference on Communications Workshops (ICC)*, pp. 1–6, IEEE, 2011.
- [22] S. Verdú, “On channel capacity per unit cost,” *IEEE Transactions on Information Theory*, vol. 36, no. 5, pp. 1019–1030, 1990.
- [23] L. Falconetti, P. Frenger, H. Kallin, and T. Rimhagen, “Energy efficiency in heterogeneous networks,” in *Online Conference on Green Communications (GreenCom)*, pp. 98–103, IEEE, 2012.
- [24] A. Fehske, G. Fettweis, J. Malmudin, and G. Biczok, “The global footprint of mobile communications: The ecological and economic perspective,” *IEEE Communications Magazine*, vol. 49, no. 8, pp. 55–62, 2011.
- [25] G. Auer, V. Giannini, C. Desset, I. Godor, P. Skillermark, M. Olsson, M. A. Imran, D. Sabella, M. J. Gonzalez, O. Blume, *et al.*, “How much energy is needed to run a wireless network?,” *IEEE Wireless Communications*, vol. 18, no. 5, pp. 40–49, 2011.
- [26] N. Docomo, “R1-114336 eNB power model.” http://www.3gpp.org/ftp/tsg_ran/wg1_r11/TSGR1_67/Docs/, 2011. Accessed: 2014-05-20.
- [27] G. Auer *et al.*, “INFSO-ICT-247733 EARTH energy efficiency analysis of the reference systems, areas of improvements and target breakdown.” http://ec.europa.eu/information_society/apps/projects/logos/

- 3/247733/080/deliverables/001_EARTHWP2D23v2.pdf, 2010. Accessed: 2014-03-16.
- [28] H. Claussen, I. Ashraf, and L. T. Ho, “Dynamic idle mode procedures for femtocells,” *Bell Labs Technical Journal*, vol. 15, no. 2, pp. 95–116, 2010.
- [29] P. Mörters and Y. Peres, *Brownian motion*, vol. 30. Cambridge University Press, 2010.
- [30] P. Révész, *Random walk in random and non-random environments*. World Scientific, 2005.
- [31] Qualcomm, “A comparison of LTE-Advanced HetNets and WiFi, whitepaper.” <http://www.qualcomm.com/media/documents/comparison-lte-advanced-hetnets-and-wifi>, 2011. Accessed: 2014-05-15.
- [32] “3GPP TR 36.842 study on small cell enhancements for E-UTRA and E-UTRAN; higher layer aspects (release 12).” <http://www.3gpp.org/DynaReport/36842.htm>, 2013. Accessed: 2014-04-11.
- [33] H. El-Shaer, “Interference management in LTE-Advanced heterogeneous networks using almost blank subframes,” Master’s thesis, KTH Vetenskap OCH Konst, Sweden, 2012.